

pubs.acs.org/joc Article

## Liberating the Anion: Evaluating Weakly Coordinating Cations

Stephen H. Dempsey and Steven R. Kass\*



Cite This: J. Org. Chem. 2022, 87, 15466–15482



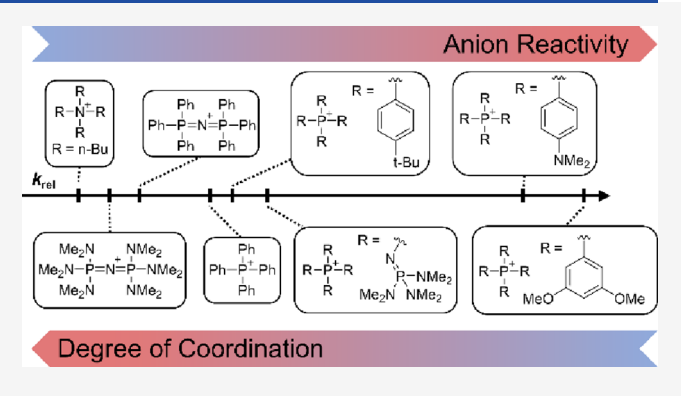
**ACCESS** I

Metrics & More

Article Recommendations

Supporting Information

**ABSTRACT:** A series of commonly used weakly coordinating cations (WCCs) including tetraalkylammonium, bis-(triphenylphosphine)iminium (PPN), P2 and P5 phosphazenium, and tetraphenylphosphonium ions were investigated along with five additional tetraarylphosphonium ions [Ar = 4-Me, 4-t-Bu, 3,5-Me<sub>2</sub>, 4-Me<sub>2</sub>N, and 3,5-(MeO)<sub>2</sub> phenyl derivatives]. Dissociation enthalpies of their chloride complexes were computed in the gas phase and in dichloromethane. These results are compared to infrared spectra of these salts in chloroform-*d* which provide free and bound C–D stretches, <sup>19</sup>F NMR spectra of the corresponding tetrafluoroborate salts, ion-pair equilibrium constants, and reaction rates of the chlorides and acetates with 1-iodooctane. The latter transformation was also carried out under catalytic conditions.



Substituted tetraphenylphosphonium ion derivatives are found to be surprisingly good WCCs that function as well or better than the P2 and P5 phosphazenium ions, the current WCC gold standard.

#### INTRODUCTION

Pairing cations with weakly coordinating anions (WCAs) has given access to remarkably reactive species. 1-3 Extensive studies with WCAs have led to potent transition-metal complexes and electrophiles and have enabled new transformations to be carried out that were previously unknown. For example, silylium cations paired with carborane anions are capable of hydrodefluorination of perfluoroalkyl groups, 4 vinyl cations exhibit surprising reactivity when paired with a WCA, 5,6 and lithium 7 and zinc 8 ions can function as much more powerful Lewis acids than when associated with more coordinating anions.

While the reactivity of a cation can give a good idea about the degree of coordination with its counteranion, structural and spectroscopic studies have also been carried out to assess the relative coordinating abilities of WCAs. For example, Reed's carborane work employed a variety of methods for comparing WCAs by pairing them with specific cationic probes. These included X-ray crystallography of metalloporphyrin salts that displayed characteristic distances depending upon the coordinating ability of the anion, 9,10 infrared (IR) spectroscopy of cyclopentadienyliron dicarbonyl and trialkylammonium salts that undergo systematic band shifts upon varying the nature of the anion, 11,12 and 13C and <sup>29</sup>Si NMR spectroscopy where the chemical shift changes with the counteranion. 12,13 More recently, Müllen et al. utilized conductance measurements to evaluate the small degree of coordination with nanometer-sized dendritic borate anion salts. These efforts and many others have facilitated the development of reactive cations and more effective WCAs.

The literature is comparatively sparse when it comes to the opposite situation, the development of weakly coordinating cations (WCCs). Nevertheless, one would expect that these ions will have a myriad of uses including the preparation of more reactive anionic nucleophiles and bases and the isolation and characterization of new metal complexes. This conclusion is based in large part on crown ethers, 15,16 cryptands and the like, 17-19 as well as the work of Schwesinger et al., who found that the fluoride anion is much more reactive when paired with P2  $[((Me_2N)_3P)_2N^+]$  and P5  $[((Me_2N)_3P=N)_4P^+]$  phosphazenium ions rather than tetraalkylammonium ions and other cations used in commercially available fluoride salts. 20,21 This class of WCCs has been exploited in the organometallic literature to stabilize reactive anionic transition-metal complexes such as the bimetallic Ni/Fe species reported by Lu et al. 22,23 and has provided a basis for the preparation and exploration of more delocalized variants. 24-26

Quantitative practical measures of coordination in synthetically relevant solvents would facilitate the development of improved WCCs and the discovery of new or further developed synthetic transformations. In this regard, we decided to evaluate some cations that are used as weakly interacting ions (1–7, Figure 1) computationally, spectroscopically,

Received: August 21, 2022 Published: November 8, 2022





Figure 1. Counterions examined in this study.

thermodynamically via their ion-pair equilibria  $(K_{\rm ip})$  and kinetically to provide a basis for the improvement of WCCs and to develop a facile method for predicting relative anion reactivities in salts with different cations. These counterions were chosen due to their widespread use in a variety of research areas (e.g., electrochemistry, organometallic complexes, and anion molecular recognition studies) and commercial availability. The information gained through this process also led us to prepare and investigate several new tetraarylphosphonium ions (i.e., 8–12).

#### RESULTS AND DISCUSSION

**Calculation of Coordination Enthalpies.** Geometries for cations 1–12 and their chloride salts were fully optimized with the M06-2X<sup>27–29</sup> density functional and the small but efficient 3-21G basis set.<sup>30</sup> The resulting low-energy structures were reoptimized with the larger and more flexible cc-pVDZ or augcc-pVDZ basis sets (see the Supporting Information),<sup>31</sup> and then their vibrational frequencies were computed to ensure that each species corresponds to an energy minimum and to provide thermodynamic information [zero-point energies (ZPEs), thermal corrections to the enthalpies, and entropies]. Gas-phase dissociation enthalpies of the chloride complexes at 298 K (MCl  $\rightarrow$  M<sup>+</sup> + Cl<sup>-</sup>  $\Delta H_{\rm rxn}$ ° =  $\Delta H_{\rm D}$ °) were calculated as shown in eq 1 and are summarized in Table 1.<sup>32</sup> Single-point

Table 1. Computed Cluster Dissociation Enthalpies at 298 K in kcal  $\mathrm{mol}^{-1}$ 

| cation | abbreviation                             | $\Delta H_{ m D}^{\circ}$ | $\Delta H_{\mathrm{D}}^{\circ} \; (\mathrm{DCM})$ |
|--------|--|---------------------------|---|
| 1      | TMA                                      | 98.8                      | 13.0  |
| 2      | TEA                                      | 93.3                      | 12.0  |
| 3      | TBA                                      | 88.9                      | 10.6  |
| 4      | P2                                       | 83.1                      | 5.7   |
| 5      | PPN                                      | 78.0                      | 8.1   |
| 6      | P5                                       | 69.4                      | 3.0   |
| 7      | $\mathrm{PPh}_4$                         | 80.9                      | 7.5   |
| 8      | 4-MePhos                                 | 77.0                      | 7.3   |
| 9      | 4-t-BuPhos                               | 75.5                      | 7.6   |
| 10     | 3,5-Me <sub>2</sub> Phos                 | 80.5                      | 8.5   |
| 11     | 4-Me <sub>2</sub> NPhos                  | 67.8                      | 2.5   |
| 12     | 3,5-(MeO) <sub>2</sub> Phos <sup>a</sup> | 84.5 (67.3)               | 11.2(10.2)  |

"Parenthetical values correspond to the higher energy anti-anti tetraarylphosphonium ion conformer (+1.2 kcal mol<sup>-1</sup>) and its corresponding chloride salt (+18.4 kcal mol<sup>-1</sup>).

energies with the conductor-like polarizable continuum solvation model (CPCM)  $^{33,34}$  for dichloromethane (DCM) along with the aug-cc-pVTZ basis set were also carried out and are included in Table 1; Grimme dispersion corrections were also computed  $^{35}$  but had a little overall impact, and the results are provided in the Supporting Information. Additional functionals ( $\omega$ B97X-D,  $^{36}$ M11,  $^{37}$  and MN15  $^{38}$ ) were explored as well, and the  $\Delta H_{\rm D}{}^{\circ}$  energies are given in the Supporting Information since they are linearly related to the M06-2X values

$$\Delta H_{\rm D}^{\circ} = \Delta H_{\rm M^+}^{\circ} + \Delta H_{\rm Cl^-}^{\circ} - \Delta H_{\rm MCl}^{\circ} \tag{1}$$

Chloride salt geometries were initially explored using chemical intuition to inform the placement of the chloride anion and then investigated from semirandom starting points. That is, Cl<sup>-</sup> was first situated so that it would adopt a favorable hydrogen bonding arrangement, and then multiple starting structures with the chloride placed 4–10 Å away from the formal charged phosphorous center were also examined. This optimization procedure led to C–H····Cl<sup>-</sup> hydrogen bonds with the hydrogens near the nominal charge center in all of the structures. The number, bond length, and orientation of these hydrogen bonds appear to be the dominant factors contributing to the chloride anion complexation energy of each cation.

As expected, tetraalkylammonium cations 1-3 with longer alkyl chains are more weakly coordinating with Cl-. Both tetramethyl- and tetraethylammonium ions have the same hydrogen bond motifs consisting of one hydrogen on three of the four  $\alpha$ -carbons to nitrogen (i.e., the formal positive charge center) serving as hydrogen bond donors. This was found to afford C-H···Cl<sup>-</sup> interactions with distances of 2.32-2.38 Å (Figure 2). In tetrabutylammonium chloride, the lowest energy complex was found to have two  $\alpha$ - and  $\beta$ -C-H hydrogen bonds (Figure 3). In this structure, the chloride anion sits in a "pocket" between two of the *n*-butyl arms and has hydrogen bond distances of 2.64 ( $\alpha$ ) and 2.68 ( $\beta$ ) Å. This complex is different from the "tilted" geometry reported by Fry which has three  $\alpha$ -C-H···Cl<sup>-</sup> interactions,<sup>39</sup> but this is not entirely surprising since the earlier study used a different functional (B3LYP) and a smaller 6-31+G(d) basis set that does not include p-orbitals on hydrogen atoms. These latter polarization functions, however, are very important for computing the geometries and energies of compounds with hydrogen bonds.40,41

Upon reoptimizing the "tilted" conformer with the 6-31+G(d) basis set [i.e., M06-2X/6-31+G(d)] its relative enthalpy at 298 K switched from +1.9 to -1.5 kcal  $mol^{-1}$ , demonstrating the favorability of the "tilted" structure in the absence of the p-orbitals on hydrogen atoms irrespective of the two density functionals.

Tetraalkylammonium ions are commonly employed as WCCs, but they can act as hydrogen bond donors, and red shifts to lower frequencies upon interactions with Brønsted bases such as pyridine and acetonitrile (ACN) have been observed in their IR spectra. They also have been shown to be capable of functioning as hydrogen bond catalysts, to but less interacting cations such as the tetraphenylphosphonium, bis(triphenylphosphine)iminium (PPN), and the P2 and P5 phosphazenium ions developed by Schwesinger are widely used and commercially available as well. These latter species have smaller computed chloride dissociation energies due to a combination of increased steric bulk, resonance

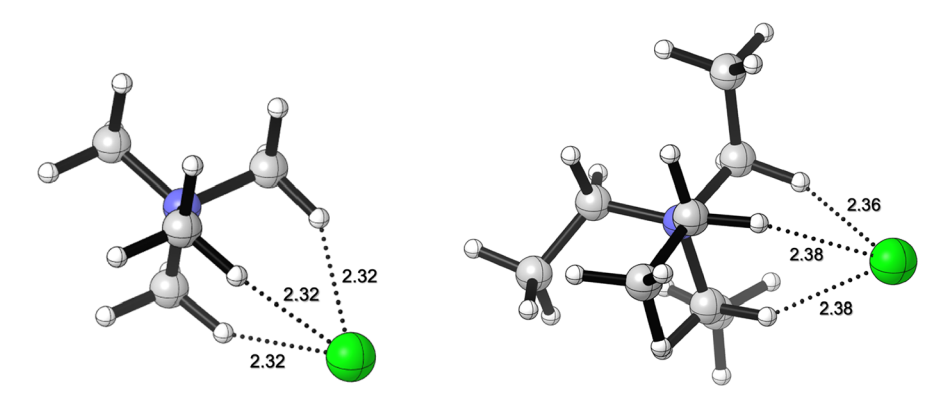


Figure 2. M06-2X/aug-cc-pVDZ optimized geometries of tetramethylammonium (1, left) and tetraethylammonium (2, right) chlorides. Distances are in Angstroms.

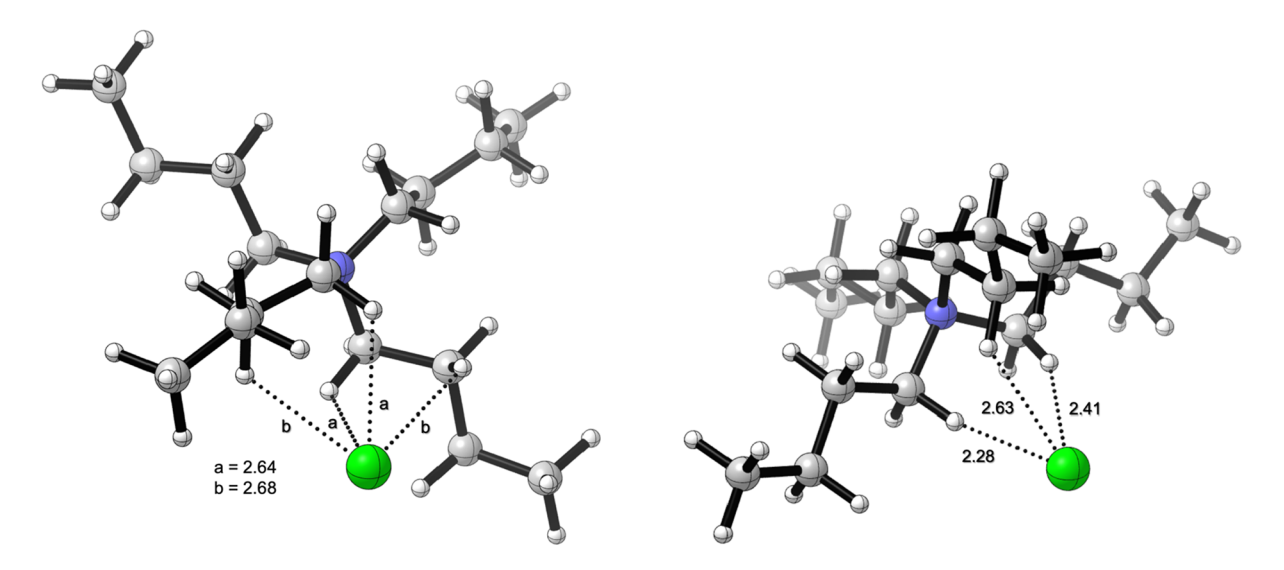


Figure 3. M06-2X/aug-cc-pVDZ optimized geometries of tetrabutylammonium chloride (3) in its more stable "pocket" (left) and less stable "tilted" (right) forms. Distances are in Angstroms.

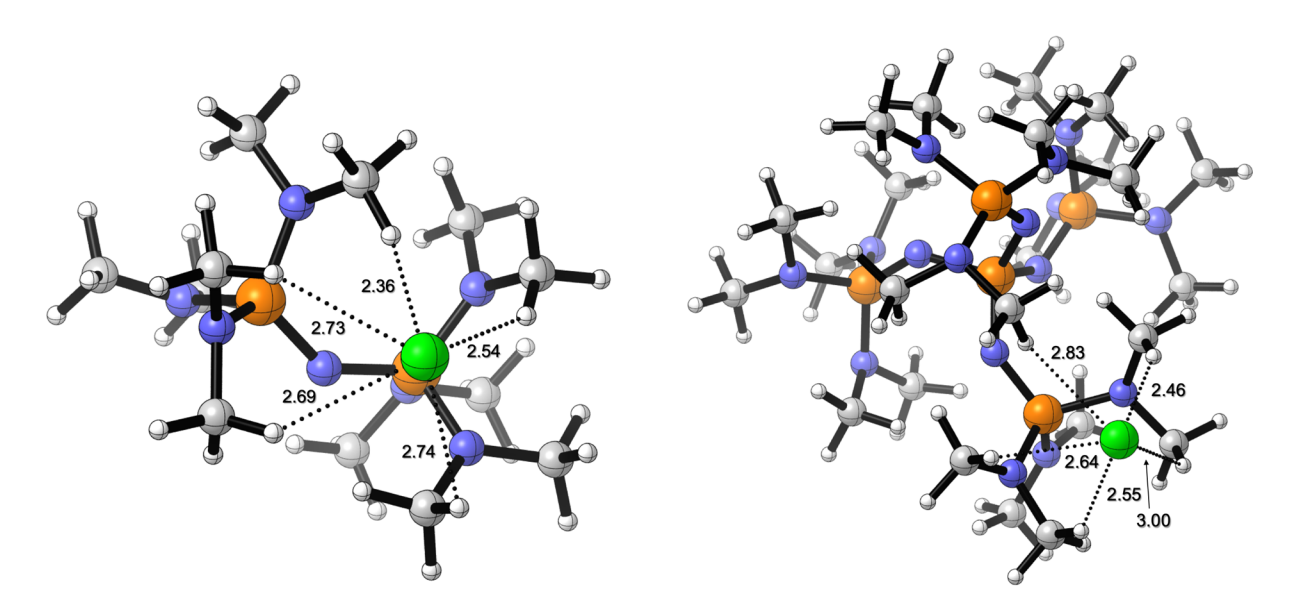


Figure 4. M06-2X/aug-cc-pVDZ optimized geometries of P2 (4, left) and P5 chlorides (6, right). Distances are in Angstroms.

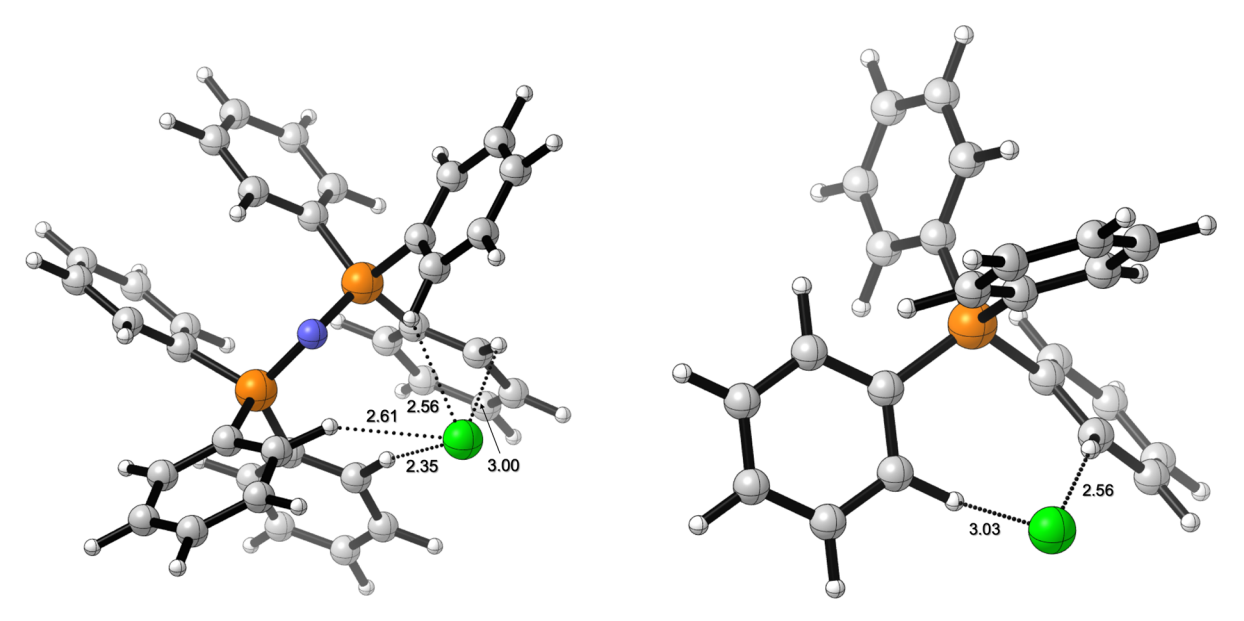


Figure 5. Computed M06-2X/aug-cc-pVDZ structures of PPN (5, left) and PPh<sub>4</sub> chlorides (7, right). Distances are in Angstroms.

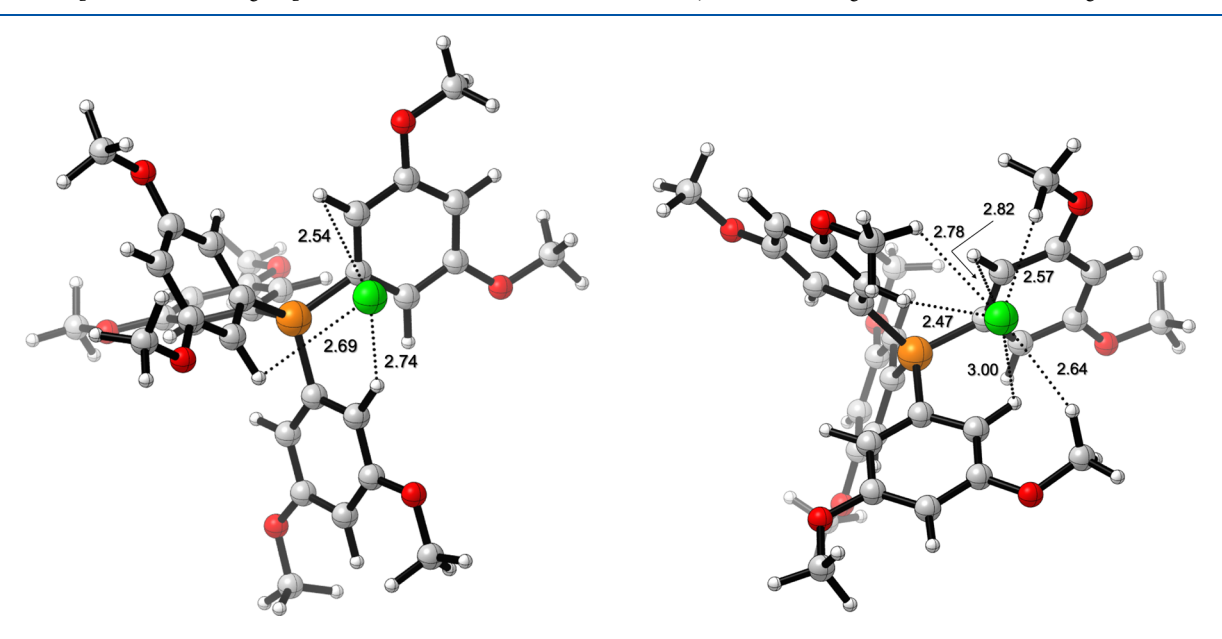


Figure 6. Computed anti-anti (left) and anti-syn (right) tetra(3,5-dimethoxyphenyl)phosphonium chloride (12) conformers. The former structure has three o-C-H····Cl $^-$  interactions, whereas the latter has an additional three OCH $_2$ -H····Cl $^-$  hydrogen bonds. Distances are in Angstroms.

electron delocalization or a difference in the nominal charge center (i.e., nitrogen vs phosphorous), and reduced hydrogen bonding abilities due to the absence of  $\alpha$ -C-H bonds. The P2 and P5 salts have similar computed C-H···Cl<sup>-</sup> hydrogen bond lengths (Figure 4), suggesting that the large difference in their complexation energies is predominantly due to the greater degree of charge delocalization in the P5 cation and the resulting increase in the distance between the chloride ion and the nominal charge center.

Analogous to the P2 salt, PPN chloride has a bent P=N=P bond (137.3 and 129.6°, respectively) with four C-H···Cl<sup>-</sup> interactions involving an *ortho*-hydrogen on four separate phenyl rings (Figure 5). Tetraphenylphosphonium ion is slightly more coordinating than PPN in the gas phase (80.9 vs  $78.0 \text{ kcal mol}^{-1}$ ) but less coordinating in DCM (7.5 vs  $8.1 \text{ kcal mol}^{-1}$ ), even though the former chloride salt only has two

hydrogen bonds, one to an ortho-hydrogen on two separate rings. This change in the relative energies is reminiscent of compensation effects<sup>49</sup> and likely represents an environmentally sensitive balance resulting from fewer hydrogen bonds but a smaller charge separation distance with PPh<sub>4</sub> due to less charge delocalization compared to PPN.

The hydrogen bonding pattern in the computed structure of tetraphenylphosphonium chloride suggested that it should be possible to weaken the attraction between the oppositely charged ions by introducing substituents onto the aromatic rings to disrupt the two hydrogen bonds and the interaction of the chloride anion with the  $\pi$ -cloud of a third phenyl ring. In this regard, steric and electronic effects were explored by introducing alkyl or electron-donating groups (i.e., NMe<sub>2</sub> and OMe) at the 4- or 3,5-positions of the benzene rings. Five phosphonium ions that we anticipated could be readily

synthesized were explored (8-12), and all of them are predicted to have smaller interaction energies with  $Cl^-$  than  $PPh_4^+$ . Four of the five are also more weakly interacting than PPN, and one of the derivatives is computed to be less coordinating than the delocalized P5 phosphazenium ion. That is, the inclusion of an electron-rich dimethylamino substituent at the para position in 11 leads to the least coordinating cation examined. This result is analogous to the improvement of WCAs by the incorporation of electron-withdrawing substituents (e.g., trifluoromethyl groups in the  $BAr_4^{-F}$  anion), and indicates that tetraarylphosphonium cations can be made more weakly coordinating by adding electron-donating groups to the aromatic rings.

A similar reduction in the chloride anion dissociation enthalpy of tetra(4-dimethylaminophenyl)phosphonium chloride (11) compared to (4-tert-butylphenyl)phosphonium chloride (9) was expected for tetra(3,5-dimethoxyphenyl)phosphonium chloride (12) relative to its alkyl-substituted analogue 10, but this is not the case. Additional degrees of conformational freedom introduced by the methoxy groups in the tetra(3,5-dimethoxyphenyl)phosphonium ion lead to a variety of local minima with similar energies, and an anti-syn conformer with one methyl group oriented away from the phosphorous center and one toward it is the most stable form that we located. Its chloride salt has a surprisingly large ion separation enthalpy of 84.5 kcal mol<sup>-1</sup>, which is only exceeded by the tetraalkylammonium ions. In contrast, the slightly less stable anti-anti phosphonium ion conformer (+1.2 kcal  $\text{mol}^{-1}$ ) has the lowest  $\Delta H_D^{\circ}$  value (67.3 kcal  $\text{mol}^{-1}$ ) of any salt examined in this study. This large difference is almost entirely due to the 18.4 kcal mol<sup>-1</sup> greater stability of the antisyn chloride salt and can largely be attributed to its six C-H... Cl<sup>-</sup> interactions compared to three in the anti-anti structure (Figure 6). Solvation calculations diminish the difference between these two conformers to 2.4 kcal mol<sup>-1</sup> and reduce  $\Delta\Delta H_{\rm D}^{\circ}$  to 1.0 kcal mol<sup>-1</sup>. Overall, these results suggest that  $(3.5-(MeO)_2C_6H_3)_4P^+$  will be a more coordinating cation than Ph<sub>4</sub>P<sup>+</sup> and possibly similar to Bu<sub>4</sub>N<sup>+</sup> unless kinetic barriers enable the anti-anti conformer to form, and the gas-phase computations are a better guide to reactivity than those in DCM. This latter possibility would be in accord with our previous findings that gas-phase acidities of salts are a better indicator of their acidities and catalytic activities in nonpolar media than DMSO pKa values because electrostatic effects are the dominant interactions.<sup>50</sup>

Synthesis of the Phosphonium Ion and WCC Salts. To experimentally test our computations, phosphonium ion salts of 8–12 were synthesized in a straightforward manner as indicated in Scheme 1. That is, commercially available aryl bromides were converted to their corresponding triarylphosphines via the reactions of their Grignard reagents with phosphorous trichloride. The desired tetraarylphosphonium

Scheme 1. Synthesis of a Series of Tetraarylphosphonium Bromides, Where  $Ar = 4 \cdot MeC_6H_4$ ,  $4 \cdot t \cdot BuC_6H_4$ ,  $3,5 \cdot (Me)_2C_6H_3$ ,  $4 \cdot Me_2NC_6H_4$ , and  $3,5 \cdot (MeO)_2C_6H_3$ 

bromides were subsequently produced by palladium coupling of each triarylphosphine with the corresponding aryl bromide. Anion interchange of the resulting salts was then carried out via anion metathesis or ion exchange chromatography. Additional species of interest are commercially available but not necessarily with the anion of interest. In these cases, ion exchange was carried out using one of the two noted approaches, and in this way, a series of acetate, chloride, and tetrafluoroborate salts were obtained. The latter two types of compounds were subsequently dried under vacuum at room temperature, whereas the acetates, which are very hygroscopic, needed to be heated to 45 or 60 °C. This unfortunately led to the decomposition of the 8–12 acetates.

Spectroscopic Characterization of Coordination. With the results from the computational exploration and a variety of salts for each cation in hand, we sought to develop a rapid and reproducible spectroscopic measure of cation coordination. We took inspiration from our previous work using solution-state IR spectroscopy to characterize acid catalysts. 50 In this approach, a dilute carbon tetrachloride solution containing a hydrogen bond donor (i.e., various phenols) was examined and the change in the phenolic O-H stretching frequency upon the addition of a small amount of a hydrogen bond acceptor (i.e., CD<sub>3</sub>CN) was found to correlate with the compound's gasphase acidity better than the DMSO pKa. It was also an effective predictor of catalyst activity in nonpolar solvents. An analogous experiment for quantifying cation coordination consequently was envisioned in which cyclohexanol serves as a hydrogen bond donor and the chloride salts as the hydrogen bond acceptor.

Our chloride salts are poorly soluble in  $CCl_4$ , and no measurable difference in the O–H stretching frequency of cyclohexanol was observed in tetrahydrofuran (THF),  $CD_2Cl_2$ , or  $CDCl_3$ . In the last of these solvents, however, a second band due to the C–D stretch was observed. It is also present in the absence of cyclohexanol, the band position varies with the cation (Figure 7), and so we attribute this feature to a C–D···  $Cl^-$  interaction. A series of salts, consequently, were examined, and the results are given in Table 2. The C–D frequency shift in going from free  $CDCl_3$  to  $MCl···D-CCl_3$  ( $\Delta\nu$ ) is largest for the tetrabutylammonium ion and smallest for the P5 phosphazenium cation. This is the opposite of what we

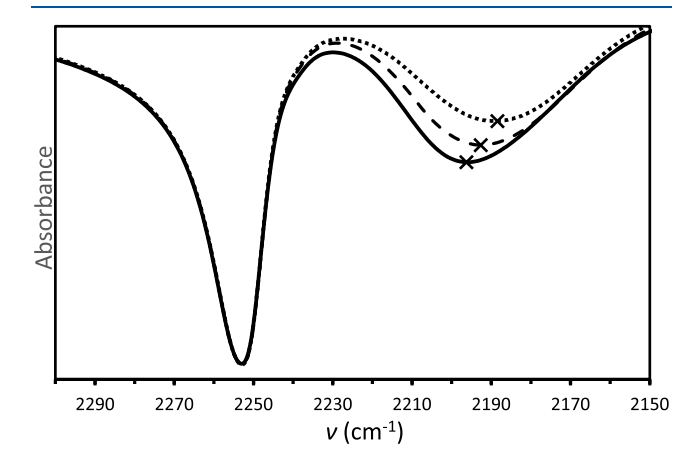


Figure 7. IR spectra in the C–D stretching region of 50 mM solutions of  $M^+$  Cl $^-$  [ $M^+$  = TBA (dotted), PPh $_4$  (dashed), and P5 (solid)] in CDCl $_3$  recorded with a 0.1 mm pathlength solution cell with NaCl windows.

Table 2. IR and <sup>19</sup>F NMR Data for a Series of Chloride and Tetrafluoroborate Salts, Respectively

| cation | abbreviation                | $\Delta v^a$ | <sup>19</sup> F NMR <sup>b</sup> |
|--------|-----------------------------|--------------|----------------------------------|
| 3      | TBA                         | 64.2         | -151.98                          |
| 4      | P2                          | 61.1         | -153.41                          |
| 5      | PPN                         | 58.9         | -153.44                          |
| 6      | P5                          | 57.3         | -153.47                          |
| 7      | $\mathrm{PPh}_4$            | 60.4         | -153.34                          |
| 8      | 4-MePhos                    | 58.2         | -153.40                          |
| 9      | 4- <i>t</i> -BuPhos         | 59.4         | -153.48                          |
| 10     | 3,5-Me <sub>2</sub> Phos    | 59.1         | -153.45                          |
| 11     | 4-Me <sub>2</sub> NPhos     | 58.0         | -153.50                          |
| 12     | 3,5-(MeO) <sub>2</sub> Phos | 60.2         | -153.38                          |
|        |                             |              |                                  |

<sup>a</sup>The change in frequency ( $\Delta \nu$ ) is given as the difference between the free C–D stretch of chloroform (i.e., 2253 cm<sup>-1</sup>) and its value in the presence of 50 mM MCl. <sup>b</sup>NMR chemical shifts of 50 mM MBF<sub>4</sub> solutions in CD<sub>2</sub>Cl<sub>2</sub> and internally referenced to fluorobenzene (–113.90 ppm).

expected since it was assumed that Cl would be freer and interact more strongly with CDCl<sub>3</sub> when paired with a more weakly coordinating cation. This suggests that a compensating effect is involved, and the chloride anion may be solvated to a greater extent when paired with a weaker interacting counterion. In accord with this possibility, M06-2X/aug-ccpVDZ computations indicate that the C-H stretching frequencies in  $Cl^{-}\cdots(H-CCl_3)_n$  increase with n and quickly approach the value for uncomplexed CHCl<sub>3</sub> (i.e., the computed unscaled average frequencies for n = 1-5 are 2700, 2928, 3049, 3104, and 3155 cm<sup>-1</sup> and that for free CHCl<sub>3</sub> is 3209 cm<sup>-1</sup>). A reasonable linear correlation is found between the computed gas-phase chloride dissociation enthalpies and the observed D-CCl<sub>3</sub> frequency shifts  $[\Delta H_D^{\circ}]$ (kcal mol<sup>-1</sup>) =  $2.87 \times \Delta \nu$  (cm<sup>-1</sup>) - 92.8,  $r^2 = 0.75$ ] and this improves considerably if one excludes the synthesized tetraarylphosphonium ions 8-12 (Figure 8). This may be the result of steric and electronic inhibition of solvation or aggregation leading to differential behavior of the related series of compounds. Differences of this sort are expected across different cation classes, suggesting that this straightforward approach provides a reasonable indication of the interaction between oppositely charged ions in a salt.

A second spectroscopic approach analogous to Reed's <sup>29</sup>Si NMR work with carboranes<sup>13</sup> was investigated for the rapid assessment of WCCs. That is, the <sup>19</sup>F NMR spectra of a series of tetrafluoroborate salts were recorded in CD2Cl2 at a concentration of 50 mM with an internal reference (Table 2). The chemical shift range is very small (0.16  $\delta$  ignoring the tetrabutylammonium salt) and leads to more scatter than the IR method noted above [i.e.,  $\Delta H_D^o$  (kcal mol<sup>-1</sup>) = 83.7 × <sup>19</sup>F NMR (ppm) + 71.6,  $r^2 = 0.57$  with the omission of TBABF<sub>4</sub>]. If one omits the tetraphenylphosphonium salt and its alkylsubstituted aryl ring variants (i.e., 7-10) from the linear leastsquare analysis, one obtains  $\Delta H_{\rm D}^{\circ}$  (kcal mol<sup>-1</sup>) = 157.0 × <sup>19</sup>F NMR (ppm) + 67.1,  $r^2 = 0.94$  (Figure 9). This could be due to the more charge-localized nature of tetraphenylphosphonium ion (7) and its alkyl derivatives 8-10, but in any case, this method holds promise even though it currently does not appear to be as reliable as the IR approach.

**Kinetics.** Given our computational and spectroscopic results, we hypothesized that the reactivity of the same anion with different WCCs is proportional to the degree of coordination. To evaluate this proposal, the  $S_N2$  reaction of 1-iodooctane with the chloride salts of 3–7, 9–12, and the protonated P4-t-Bu phosphazene base (13) was examined under pseudo-first-order conditions (eq 2). Observed rate

constants were determined via nonlinear least-square fits of the absorbances of the iodide salt products at 367 nm except for  $(3,5\text{-}(\text{MeO})_2\text{C}_6\text{H}_4)_4\text{PCl}$ , where it corresponded to the starting chloride salt, and P5Cl (Table 3). In this latter case, the reaction was monitored by  $^1\text{H}$  NMR because a Beer's law plot of the P5 iodide is distinctly nonlinear with the absorbance plateauing around the concentration that would correspond to 80% conversion, and the UV kinetic trace displays two inflection points. The NMR data are well-behaved, and none of the other species exhibit this behavior. We hypothesize that an aggregate of the P5 iodide has a lower molar absorptivity than the monomer (or a smaller aggregate), and this could lead to the observed decrease in absorptivity with its increase in

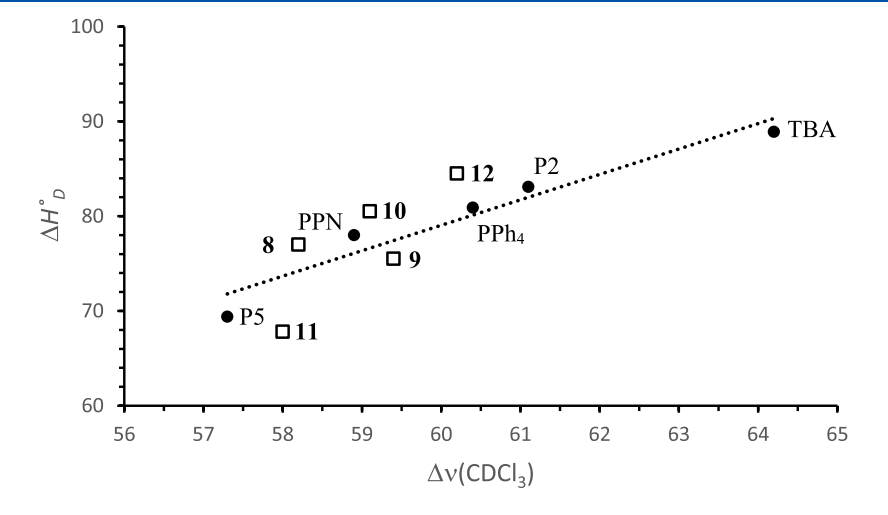


Figure 8. Linear correlation of  $\Delta H_{\rm D}^{\circ}$  (MCl) vs  $\Delta \nu$  (CDCl<sub>3</sub>) for the chloride salts of TBA, P2, PPN, P5, and Ph<sub>4</sub>P (3–7);  $\Delta H_{\rm D}^{\circ}$  (kcal mol<sup>-1</sup>) = 2.68  $\times \Delta \nu$  (cm<sup>-1</sup>) – 81.9,  $r^2$  = 0.94. Open squares correspond to 8–12 and are omitted from the linear fit.

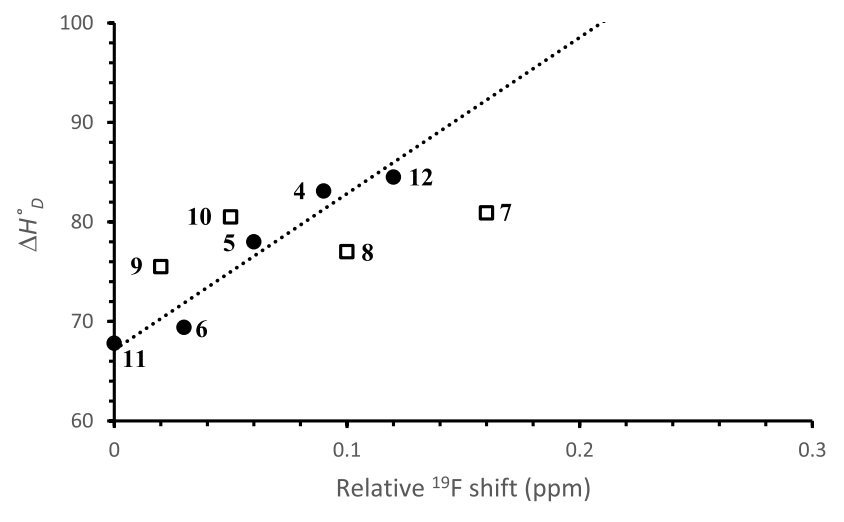


Figure 9. Linear correlation of  $\Delta H_D^o$  (MCl) vs relative <sup>19</sup>F NMR shift (ppm) for the tetrafluoroborate salts of 4–6, 11, and 12. Open squares are omitted from the linear fit and correspond to 7–10.

Table 3. Pseudo-First-Order Kinetic Results for the  $S_{\rm N}2$  Reaction of 1-Iodooctane with a Series of Chloride Salts and Their Ion-Pairing Equilibrium Constants<sup>a</sup>

| cation                        | $k \text{ (min}^{-1})$ | $k_{ m rel}$ | $K_{\rm ip}~({ m M}^{-1})$ |
|-------------------------------|------------------------|--------------|----------------------------|
| TBA (3)                       | 0.00128                | 1.00         | $4.37 \times 10^4$         |
| P2 (4)                        | 0.00409                | 3.20         | $6.00 \times 10^{3}$       |
| PPN (5)                       | 0.00411                | 3.21         | $9.01 \times 10^{2}$       |
| PPh <sub>4</sub> (7)          | 0.00677                | 5.29         | $2.64 \times 10^{3}$       |
| P4-t-Bu·H (13)                | 0.0135                 | 10.5         |                            |
| 3,5-Me <sub>2</sub> Phos (10) | 0.0154                 | 12.0         | $2.28 \times 10^{3}$       |
| P5 (6) <sup>b</sup>           | 0.0185                 | 14.5         | $1.17 \times 10^{5}$       |
| 4- <i>t</i> -BuPhos (9)       | 0.0186                 | 14.5         | $6.86 \times 10^{2}$       |
| 4-Me <sub>2</sub> NPhos (11)  | 0.0419                 | 32.7         | $8.87 \times 10^{2}$       |
| $3.5 - (MeO)_2 Phos (12)^c$   | 0.0472                 | 36.9         | $5.66 \times 10^{2}$       |

"Reactions monitored at 367 nm by UV—vis spectroscopy in  $CH_2Cl_2$  at 25 °C unless otherwise noted. NMR titrations with salt concentrations of ~0.05–25 mM were carried out, and the resulting data were fit using the BindFit app dimerization model to obtain the  $K_{\rm ip}$  values (app.supramolecular.org/bindfit, refs 51 and 52). Beaction monitored by <sup>1</sup>H NMR spectroscopy and the rate constant was obtained from a linear fit of the data. In this case, the absorbance at 367 nm corresponds to the disappearance of the starting chloride salt.

concentration. Further investigation would be needed to address this issue but is beyond the scope of this study.

Tetrabutylammonium chloride is the least reactive salt examined, which is consistent with our computations and spectroscopic data, as well as previous observations showing that tetrasubstituted ammonium ions can function as hydrogen bond catalysts. 45-47 PPN and the P2 phosphazenium ions are both three times more reactive than the TBA salt (i.e.,  $k_{rel} = 3.2$ in both cases) but a little slower than tetraphenylphosphonium chloride, which has a relative rate of five. These findings are in keeping with the common use of PPN and PPh4 as less coordinating ions than TBA in anion binding studies. 53-55 The larger and more delocalized conjugate acid of the P4-t-Bu phosphazene superbase is an even better cation ( $k_{rel} = 10.5$ ) despite having an N–H hydrogen that can serve as a hydrogen bond donor to the chloride anion. Elimination of this hydrogen bond donating site in the similarly large and delocalized P5 ion affords an  $\sim$ 50% improvement in the reaction rate (i.e.,  $k_{\rm rel}$  = 14.5). Surprisingly, the tetraarylphosphonium salts are very reactive. The incorporation of two methyl groups at the 3,5-positions of each aromatic ring in PPh4 leads to a more reactive salt than the P4 derivative (i.e.,  $k_{rel} = 12.0 \text{ vs } 10.5$ ), and tetra(4-t-butylphenyl)phosphonium chloride ( $k_{rel} = 14.5$ ) is as reactive as the P5 salt. Incorporating electron-donating 4-

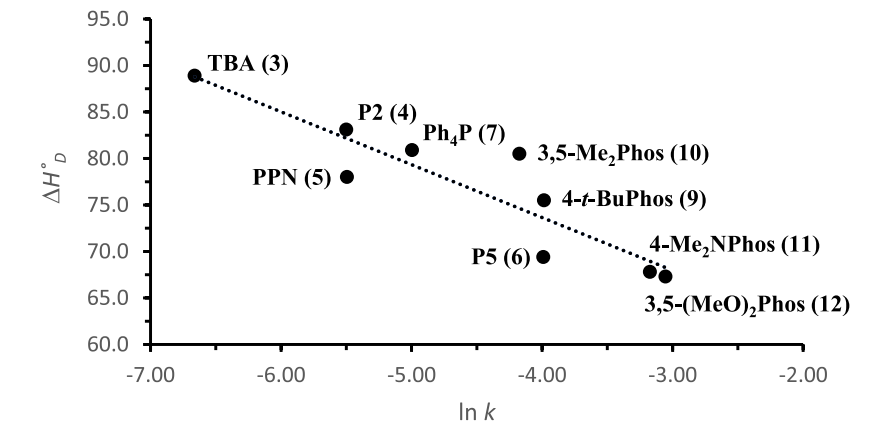


Figure 10. Linear correlation of  $\Delta H_D^c$  (MCl) vs ln k for the reaction illustrated in eq 2 using the chloride salts of 5–13, where 10 (open circle) was omitted from the least-square fit and the less stable anti–anti conformer of 12 was used.

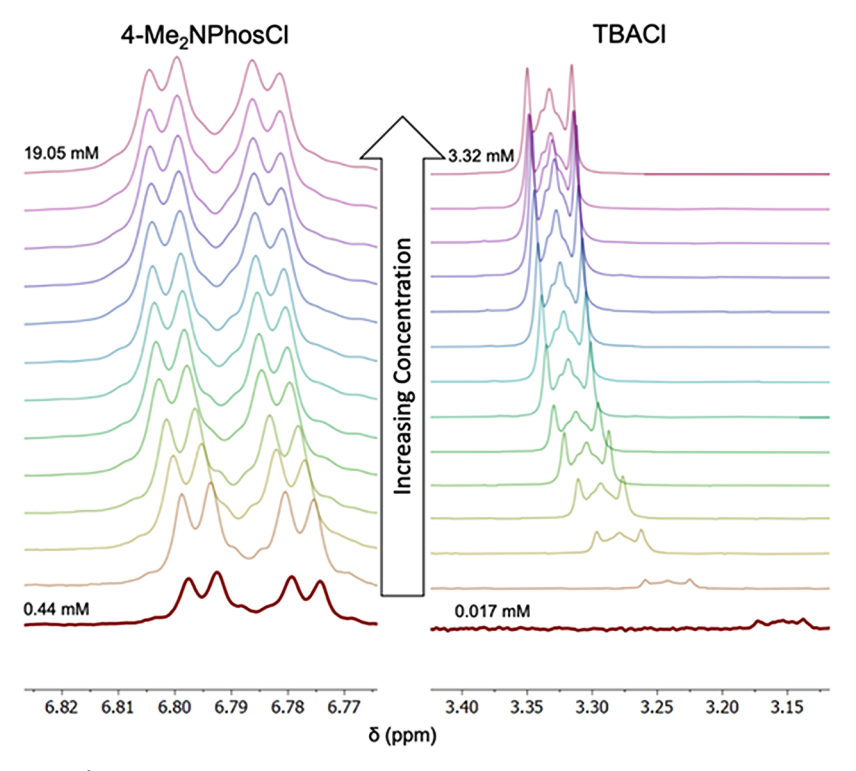


Figure 11. Illustrative examples of <sup>1</sup>H NMR spectra from titration data for relatively strong and weak interacting cations with Cl<sup>-</sup> [i.e., TBACl (right) and 4-Me<sub>2</sub>NPhosCl (left), respectively]. Good nonlinear fits of the data were obtained in both cases.

dimethylamino and 3,5-dimethoxy substituents into the phenyl rings of PPh<sub>4</sub> leads to the most reactive compounds we examined (i.e.,  $k_{\rm rel} = 32.7$  and 36.9, respectively).

A reasonable linear correlation is obtained between the computed gas-phase chloride dissociation enthalpies and the logarithm of the observed rate constants for the  $S_N2$  reaction between 1-iodooctane and chloride salts 5-13 [ $\Delta H_D^o$  (kcal mol<sup>-1</sup>) =  $-5.69 \times \ln k + 50.9$ ,  $r^2 = 0.82$ ]. All of the data points were used, but the less stable anti—anti conformer of tetra(3,5-dimethoxyphenyl)phosphonium ion (12, +1.2 kcal mol<sup>-1</sup>) and its corresponding chloride salt conformer were employed (Figure 10). Similar results were obtained with the  $\omega$ B97X-D, M11, and MN15 functionals and Grimme dispersion corrections of the M06-2X energies, as well as for the CPCM in DCM. In this last case, a satisfactory correlation was only obtained if the sterically bulky (4-t-BuC<sub>6</sub>H<sub>4</sub>)<sub>4</sub>P derivative was also excluded from the least-square analysis.

The linear correlation of  $\Delta H_{\rm D}^{\circ}$  with  $\ln k$  might not be expected given that specific solvation, aggregation, and counterion effects are not accounted for in our calculations. Salts are also known to exist in a variety of forms in organic solvents<sup>57-61</sup> including contact ion pairs (CIPs), separated ion pairs (SIPs), and free ions. 61-69 All of these species can have quite different reactivities, and based upon studies largely with alkali metal counterions, it has been reported that free ions and SIPs have similar reactivity, while CIPs are generally much less reactive. 53,61,64-69 There are relatively few reports, however, with organic cations. In one instance with PPNBr, it was found that its CIP and SIP are nearly equally reactive, further complicating the identification of the reactive species.<sup>53</sup> Differentiating the structures that salts adopt in nonpolar media is a challenging task, but to make progress in this regard, NMR dilution studies of the chloride salts 3-7 and 9-13 were

carried out in  $CD_2Cl_2$  to obtain ion-pairing equilibrium constants (eq 3).  $^{70,71}$ 

$$M^+ + Cl^- \xrightarrow{(K_{ip})} M^+ Cl^-$$
free ions CIP/SIP (3)

Satisfactory fits of the NMR data as illustrated for 4-Me<sub>2</sub>NPhosCl (11Cl) and TBACl (Figure 11) were obtained for all of the salts at low concentrations (see the Supporting Information for more details), but deviations from the binding model were observed with TBA, P2, and P5 at concentrations approaching those used in the kinetic experiments (i.e., 25 mM).<sup>72</sup> This is likely due to the formation of higher-order aggregates for P2 and P5 and the presence of more than one species, given that the change in the chemical shift plateaus during the titration and then undergoes a gradual decrease at higher concentrations. 51,57 All of the data for both phosphazenium salts are provided in the Supporting Information along with where the concentrations were truncated to obtain  $K_{ip}$ . For TBA, when higher concentrations were used (>5 mM) an unrealistic binding constant of >10<sup>16</sup> M<sup>-1</sup> was obtained. This determination was used to obtain the appropriate concentration region and is given in the Supporting Information but not used to obtain  $K_{ip}$  since binding models are known to give unreliable results when applied across inappropriate concentration ranges.<sup>51</sup> The measured K<sub>ip</sub> values (Table 3) span from 600 to 200,000 M<sup>-1</sup> with the largest ones for TBA and P5 chloride and the smallest values for the PPN and  $Ar_4P$  salts, where Ar = 4-t- $BuC_6H_4$ , 4-Me<sub>2</sub>NC<sub>6</sub>H<sub>4</sub>, and 3,5-(MeO)<sub>2</sub>C<sub>6</sub>H<sub>3</sub>). The big equilibrium constant for P5Cl presumably is not because of an especially favorable interaction between the cation and anion, but rather weak interactions between P5 and the solvent. This is analogous to Smid's explanation for CIP formation with cesium salts in THF as opposed to CIP and SIP

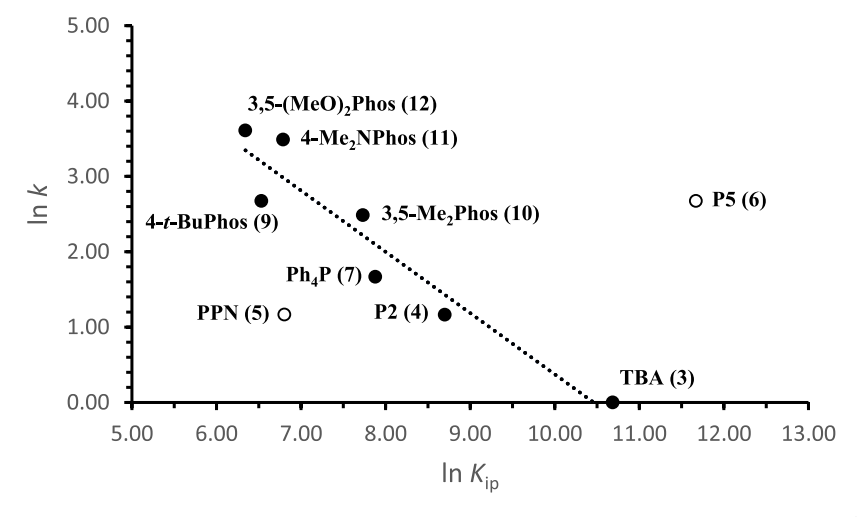


Figure 12. Linear correlation of  $\ln k_{\rm rel}$  vs  $\ln K_{\rm ip}$  for the data in Table 4, where the results for the P5 and PPN chlorides (open circles) were omitted from the least-square analysis.

mixtures with smaller alkali metals.<sup>61</sup> In spite of this, P5Cl is among the more reactive chlorides that we examined.

For each salt whose  $K_{\rm ip}$  was measured, the value is large enough such that the free ion concentration must be quite small (i.e., <1% of a rapidly equilibrating CIP/SIP and free ion mixture). Given that higher-order aggregates are also undoubtedly present and have varying reactivities, it is not surprising that  $\ln k$  and  $\ln K_{ip}$  are not well correlated.<sup>73</sup> However, a good linear fit  $[\ln k (s^{-1}) = -0.81 \times \ln K_{ip} (M^{-1}) +$ 8.50,  $r^2 = 0.906$ ] is obtained when the data for the P5 and PPN salts are omitted from the least-square analysis (Figure 12). Given that the UV-vis reactivity data for the former compound revealed the presence of at least two kinetically active species, its omission seems justified and we assume that this explanation also applies to the PPN salt. The observed log-log relationship between k and  $K_{ip}$  suggests that the greater reactivity of the substituted electron-rich phosphonium ion salts compared to tetraphenylphosphonium chloride is related to the degree of dissociation of the chloride ion pairs. 4

Reaction kinetics for select salts were also performed in ACN, but since this solvent is very polar and SIPs and/or free ions are presumably dominant, there is little difference between the most reactive ion pairs. The PPN (5), P5 (6), 3,5-(MeO)<sub>2</sub>Phos (12), and PPh<sub>4</sub> (7) chloride salts react at similar rates but about 3–4 times faster than for TBA chloride (i.e.,  $k_{\rm rel}$  = 4.0, 3.9, 3.8, 2.5, and 1.0, respectively). We therefore turned to the acetate salts and their reactions in CDCl<sub>3</sub> with 1-iodooctane (eq 4). For these faster-occurring processes, the kinetics were monitored under second-order conditions using <sup>1</sup>H NMR as the analytical method (Table 4).

Potassium acetate is not soluble in chloroform, but it dissolves in the presence of 18-crown-6, and under these conditions, it reacts with 1-iodooctane. This commonly used reagent for binding  $K^+$  and accelerating reactions of the corresponding counteranion is not as effective as any of the tetraalkylammonium ions and affords the slowest reaction rate (i.e.,  $k_{\rm rel} = 0.5$ ). Faster reactions are observed for the latter salts

Table 4. Second-Order Kinetic Results for the S<sub>N</sub>2 Reaction of 1-Iodooctane with a Series of Acetate Salts<sup>a</sup>

| cation                               | $k_{\rm obs}~(\mathrm{M}^{-1}~\mathrm{min}^{-1})$ | $k_{ m rel}$ |
|--------------------------------------|---|--------------|
| 18-crown-6·K⁺                        | 0.00134   | 0.5          |
| TMA (1)                              | 0.00285   | 1.0          |
| TEA (2)                              | 0.0104  | 3.6          |
| TBA (3)                              | 0.0328  | 11.5         |
| PPN (5)                              | 0.0832  | 29.2         |
| P2 ( <b>4</b> )                      | 0.0923  | 32.4         |
| $PPh_4$ (7)                          | 0.0956  | 33.5         |
| P5 (6)                               | 0.102   | 35.8         |
| P4- <i>t</i> -Bu·H <sup>+</sup> (13) | $0.104^{b}$                                       | 36.4         |
| K <sup>+</sup> (2.2.2-cryptand)      | $0.123^{b}$                                       | 43.3         |

<sup>a</sup>Reactions monitored by <sup>1</sup>H NMR spectroscopy in CDCl<sub>3</sub> at 25 °C and the rate constants were obtained from linear least-square fits of the resulting data. <sup>b</sup>Initial rates are given as the reaction slowed down after  $\sim$ 40–50% conversion to the product.

 $(R_4N^+\ OAc^-)$  and the relative rates increase with the size of the alkyl groups from 1.0 to 3.6 and 11.5 (i.e., R=Me, Et, and Bu, respectively). All of the other examined compounds including the 2.2.2-cryptand react about 3–4 times faster than tetrabutylammonium acetate, but the reactions with both  $K^+$  (2.2.2-cryptand) and P4-t-Bu·H $^+$  level off at  $\sim$ 50% conversion. This behavior was not expected and may be the result of a number of factors such as differential solubility, solvation, and aggregation effects of the starting bidentate acetates and monodentate iodide products.

The  $\Delta H_{\rm D}^{\circ}$  computations on the TMA (1), TEA (2), TBA (3), P2(4), PPN (5), and PPh<sub>4</sub> (7) chlorides but not the P5 (6) salt are linearly related to  $\ln k$  for the acetate salts, and the least-square analysis affords  $\ln k = -0.174$   $\Delta H_{\rm D}^{\circ} + 11.6$ ,  $r^2 = 0.925$  (Figure S15). Ion-pairing equilibrium constants for the acetate salts were not obtained even though both TBAOAc and PPh<sub>4</sub>OAc were examined. This is because different values were obtained by independently fitting the NMR shifts for the cation and anion, which indicates that the dimerization binding model is not the correct choice. This is reasonable to hypothesize that, in these instances, higher-order aggregates are present even at sub-1 mM concentrations. This tracks with our observations for the chloride salts in CDCl<sub>3</sub> and suggests that the dominant factor in this reaction may be the reactivity

of the aggregates of the acetate salts. Our experimental design, as with the chlorides, nevertheless provides a relative ranking of the different cations.

Reactivity Exploration. It has been found that one can use a catalytic amount of a WCA to promote the reactivity of electrophiles. 4,75 This suggests that a catalytic amount of a WCC could be used to enhance nucleophilic and elimination reactions. Two recent reports have demonstrated the potential of this approach by enhancing the reactivity of cesium fluoride. That is, Kondo et al. utilized CsF with a catalytic amount of P5Cl to carry out the desilylative carboxylation of aryltrimethylsilanes in the presence of  $CO_2^{76}$  and researchers at Merck used KF or CsF to carry out nucleophilic aromatic substitution reactions of aryl chlorides with TMACl as the catalyst.<sup>77</sup> We decided to apply this approach to the formation of n-octyl acetate from 1-iodooctane using a stoichiometric amount of TMAOAc and a variety of MCl salts as the catalyst (eq 5) particularly since some of the acetates are difficult to dry and undergo decomposition in the process at mild temperatures.

n-Oct 
$$\frac{M^{+}CI^{-}(10 \text{ mol}\%)}{CH_{2}Cl_{2}: Et_{2}O(1:1)}$$
 n-Oct  $0$  (5)

In DCM, tetramethylammonium acetate is sparingly soluble but undergoes a reaction with 1-iodooctane at 30 °C, leading to a 42% product conversion after 2.5 h. In the presence of 10 mol % MCl [M = PPh<sub>4</sub>, PPN, and 3,5-((MeO)<sub>2</sub>C<sub>6</sub>H<sub>3</sub>)<sub>4</sub>P], the reaction conversions increased to 62–63%, whereas in diethyl ether, no reaction with TMAOAc was observed. Subsequently, a 1:1 CH<sub>2</sub>Cl<sub>2</sub>/Et<sub>2</sub>O solvent mixture was explored because this preserved the solubility of the catalysts and largely eliminated the background process with TMAOAc (Table 5). Only a 5%

Table 5. Catalyzed  $S_N2$  Reactions of 1-Iodooctane with a Stoichiometric Amount of Tetramethyl-Ammonium Acetate and 10 mol % of a Chloride  $Salt^a$ 

| catalyst     % conversion       none     5.2       P5Cl     45.8       TBACl     55.3 $(3,5\text{-}(\text{MeO})_2\text{C}_6\text{H}_3)_4\text{PCl}$ 61.6       PPh <sub>4</sub> Cl     73.2 $(4\text{-Me}_2\text{NC}_6\text{H}_4)_4\text{PCl}$ 78.5 $(4\text{-}t\text{-BuC}_6\text{H}_4)_4\text{PCl}$ 82.8       P2Cl     85.0       PPNCl     85.4 |
|---|
| $\begin{array}{lll} P5Cl & 45.8 \\ TBACl & 55.3 \\ (3,5-(MeO)_2C_6H_3)_4PCl & 61.6 \\ PPh_4Cl & 73.2 \\ (4-Me_2NC_6H_4)_4PCl & 78.5 \\ (4-t-BuC_6H_4)_4PCl & 82.8 \\ P2Cl & 85.0 \\ \end{array}$  |
| TBACI $55.3$ $(3,5\text{-}(MeO)_2C_6H_3)_4PCI$ $61.6$ PPh <sub>4</sub> Cl $73.2$ $(4\text{-Me}_2NC_6H_4)_4PCI$ $78.5$ $(4\text{-}t\text{-Bu}C_6H_4)_4PCI$ $82.8$ P2Cl $85.0$  |
| $\begin{array}{ll} (3,5\text{-}(\text{MeO})_2\text{C}_6\text{H}_3)_4\text{PCl} & 61.6 \\ \text{PPh}_4\text{Cl} & 73.2 \\ (4\text{-}\text{Me}_2\text{NC}_6\text{H}_4)_4\text{PCl} & 78.5 \\ (4\text{-}t\text{-}\text{BuC}_6\text{H}_4)_4\text{PCl} & 82.8 \\ \text{P2Cl} & 85.0 \\ \end{array}$  |
| $\begin{array}{lll} PPh_4Cl & 73.2 \\ (4-Me_2NC_6H_4)_4PCl & 78.5 \\ (4-t-BuC_6H_4)_4PCl & 82.8 \\ P2Cl & 85.0 \end{array}$   |
| $(4-Me_2NC_6H_4)_4PCl$ 78.5<br>$(4-t-BuC_6H_4)_4PCl$ 82.8<br>P2Cl 85.0  |
| $(4-t-BuC_6H_4)_4PCl$ 82.8<br>P2Cl 85.0   |
| P2Cl 85.0   |
|   |
| PPNCI 85.4  |
| 111.61  |

"Reactions were run in a 1:1  $\rm CH_2Cl_2/Et_2O$  mixture at 30 °C over the course of 2.5 h.

conversion to n-octyl acetate was obtained without the presence of a catalyst, and this increased to 46-85% in the presence of 10 mol % of a variety of chloride salts. Side product formation of 1-chlorooctane was also insignificant in each case due to rapid salt metathesis and the greater reactivity of acetate over chloride. Interestingly, the least effective catalysts are P5Cl and TBACl, and the most active ones are  $(4-t\text{-BuC}_6\text{H}_4)_4\text{PCl}$ , P2Cl, and PPNCl. This reactivity order is not consistent with our computational or kinetic data but is in keeping with the ion-pairing equilibrium constants. While more than one factor undoubtedly is involved, free ion

reactivity and the phase transfer ability of the chloride salts appear to be critical factors in determining the reaction conversions. However, since TMAOAc is only sparingly soluble in the reaction solvent, the ability to solubilize acetate is essential and phase transfer ability alone could account for the observed reactivity order.

#### CONCLUSIONS

Full geometry optimizations of chloride salts 1Cl-12Cl revealed that hydrogens on  $\alpha$ - and  $\beta$ -carbons to the formal positive charge center function as hydrogen bond donors to the chloride anion. Multiple interactions of this sort along with  $Cl^- \cdots \pi$  interactions lead to computed dissociation enthalpies  $(\Delta H_{\mathrm{D}}^{\circ})$  that span a 30 kcal mol $^{-1}$  range. Tetraalkylammonium salts (R = Me, Et, and n-Bu, 1-3) have the largest values and interact with Cl- most strongly. In contrast, the P5 (6), 4-Me<sub>2</sub>NPhos (11), and 3,5-(MeO)<sub>2</sub>Phos (12) derivatives have the smallest  $\Delta H_{\mathrm{D}}^{\circ}$  values and are predicted to be the most weakly coordinating cations examined. These results are in reasonable accord with IR shifts of the C-D stretch of chloroform-d upon coordination with the chloride salts. An analogous spectroscopic surrogate for chloride anion complexation using <sup>19</sup>F NMR of the tetrafluoroborate salts proved to be less robust but is worth probing further. Reaction rates for the S<sub>N</sub>2 transformation of the chloride salts with 1-iodooctane in DCM also correlated well with  $\Delta H_{\rm D}^{\circ}$  and revealed that (4- $Me_2NC_6H_4$ )<sub>4</sub>PCl and  $(3.5-(MeO)_2C_6H_3)_4$ PCl react faster than P5Cl. Similar kinetic results were obtained with the acetate salts, but the dry substituted phosphonium ion derivatives proved to be relatively unstable. This presumably is due to the increased basicity of the counteranion but can be overcome by generating them in situ, and even in a catalytic fashion. As a result, substituted phosphonium ions are a promising source of WCCs. An unexpected correlation (due to the presence of CIPs, SIPs, free ions, aggregates, and other species) between ln  $K_{iD}$  for the chloride salts and  $\ln k$  for the reactions of MCl with 1-iodooctane also may facilitate the development of new and novel WCCs.

#### EXPERIMENTAL SECTION

**General.** Tetraphenylphosphonium bromide and chloride and all aryl bromides were purchased from Oakwood Chemical. Tri-ptolylphosphine was purchased from Alfa-Aesar. High-performance liquid chromatography (HPLC) grade methanol, DCM, THF, diethyl ether, and anhydrous K<sub>2</sub>CO<sub>3</sub> were purchased from Fisher Scientific. Deuterated solvents were acquired from Cambridge Isotope Laboratories. All other reagents and solvents, including Amberlite IRA-67 and Dowex Marathon A2 ion exchange resins, were purchased from Sigma-Aldrich.

Glassware was dried in an oven at 120 °C and allowed to cool while flushing it with argon. Alumina and molecular sieves were activated and stored in a kiln at 300 °C. THF was distilled from sodium and benzophenone. ACN, DCM, and CCl<sub>4</sub> were dried by passing them through activated alumina and stored over activated 3 Å molecular sieves under an argon atmosphere. m-Xylene was degassed thoroughly via several freeze–pump—thaw cycles and dried over 3 Å molecular sieves for at least 24 h. HPLC-grade methanol for ion exchanges was used as purchased. Deuterated chloroform was treated with anhydrous  $K_2CO_3$  and dried over 3 Å molecular sieves for 24 h prior to use. Deuterated DCM was dried with 3 Å molecular sieves for 24 h. Aryl bromides used in the phosphine and phosphonium ion syntheses and 1-iodooctane were purified by passing them through activated alumina, stored under argon, and used within 48 h.

NMR spectra were recorded on 400 and 500 MHz spectrometers. Chemical shifts are given in ppm and were referenced as follows:  $\delta$ 

7.27 (CDCl<sub>3</sub>,  ${}^{1}$ H):  $\delta$  77.0 (CDCl<sub>3</sub>,  ${}^{13}$ C):  $\delta$  5.32 (CD<sub>2</sub>Cl<sub>2</sub>,  ${}^{1}$ H)  $\delta$  2.05 (acetone- $d_6$ , <sup>1</sup>H),  $\delta$  –78.5 (<sup>19</sup>F, CF<sub>3</sub>CO<sub>2</sub>H, external calibrant). <sup>31</sup>P shifts were referenced through the deuterium lock channel according to the IUPAC unified scale. <sup>78</sup> For BF<sub>4</sub> salts, <sup>19</sup>F NMR spectra were recorded with fluorobenzene as an internal reference set to -113.90ppm, in accordance with a recent study on the irreproducibility of fluorine NMR chemical shifts.  $^{79}$   $^{1}\mathrm{H}$  NMR spectra for the acetate salts were taken with a 10 s relaxation delay to give more accurate integrations. Uncorrected melting points were determined using sealed tubes. High-resolution mass spectra were collected using an electrospray ionization (ESI) time-of-flight instrument using methanolic solutions and polypropylene glycol (PPG) as an internal calibrant. Fourier transform IR spectra were recorded with a laminated diamond attenuated total reflection (ATR) attachment for all solid samples and a transmission cell with NaCl windows and a 0.1 mm path length for the liquid-phase studies. For solid samples, nondiagnostic IR bands above 3200 cm<sup>-1</sup> were excluded since many of the species were quite hygroscopic and spectra were recorded in the open. UV-vis kinetic data were collected using a spectrometer equipped with an eight-cell Peltier temperature-controlled apparatus. Threaded 10 mm quartz cuvettes equipped with Mininert caps were used in all cases to ensure an inert and moisture-free atmosphere over the course of the reactions. The cuvettes were sealed with electrical tape and parafilm as an added precaution.

Preparation of Acetate Ion Exchange Column. An acetate ion exchange column (2 cm diameter, 40 cm height) was prepared from the chloride form of Dowex Marathon A2 (also known as AmberLite HPR4100) strongly basic ion exchange resin. This was done by first converting the resin to its hydroxide form by passing 400 mL of a 2 M NaOH solution through the column over the course of 1 h. The column was then rinsed with deionized water until the eluent had a pH of 7. Dilute acetic acid (10% v/v) was subsequently passed through the column, and residual acetic acid and salts were removed by rinsing it with deionized water until the eluent had a neutral pH. To prepare for ion exchange, the column was thoroughly rinsed with water and left submerged for at least 2 h before use. It was then used up to five times before being regenerated by the above method. The resin bed was regenerated 10 times before any loss in performance could be observed at which point it was remade.

General Procedure for the Synthesis of Acetate Salts. The organic chloride, bromide, or tetrafluoroborate salt (1 equiv) was dissolved in a minimal amount of water (unless otherwise specified) and transferred to the ion exchange column (2 × 40 cm, ≫10 equiv). Approximately 300 mL of water was passed through the column and collected. The solvent was removed on a rotary evaporator, and 50 mL of benzene was added to the residue and removed to azeotrope off residual water. This latter process was repeated two additional times, and the resulting sticky solid was dried under vacuum (<0.1 Torr) for 24−72 h at the specified temperature to afford the acetate salt. The resultant hygroscopic salts were transferred into a nitrogen glovebox for storage.

Tetramethylammonium Acetate (10Ac). <sup>80</sup> Tetramethylammonium chloride (2.00 g, 18.2 mmol, 1.0 equiv) afforded 2.23 g (92%) of its acetate salt as a very hygroscopic white solid using the general procedure. It was then dried under vacuum (<0.1 Torr) for 48 h at room temperature. <sup>1</sup>H NMR (400 MHz, (CD<sub>3</sub>)<sub>2</sub>CO): δ 3.45 (s, 12H), 1.76 (s, 3H). Note—this compound is commercially available.

Tetraethylammonium Acetate (20Ac).<sup>81</sup> Tetraethylammonium chloride (520 mg, 3.13 mmol, 1.0 equiv) afforded 566 mg (95%) of the acetate salt as a thick clear oil via the general procedure. The oil was dried under vacuum (<0.1 Torr) for 48 h at 50 °C and thickened to a waxy off-white solid. <sup>1</sup>H NMR (400 MHz, CDCl<sub>3</sub>):  $\delta$  3.43 (q, J = 7.3 Hz, 8H), 1.90 (s, 3H), 1.34 (t, J = 7.3, 12H). Note—this compound is commercially available as the pentahydrate.

Tetraphenylphosphonium Acetate (70Ac). <sup>82</sup> Tetraphenylphosphonium bromide (350 mg, 0.83 mmol, 1 equiv) dissolved in 1:1 methanol/water afforded 319 mg (96%) of the acetate salt as a white solid using the general procedure. The resulting powder was dried under vacuum (<0.1 Torr) for 24 h at room temperature (mp 220–225 °C with decomp). <sup>1</sup>H NMR (500 MHz, CDCl<sub>3</sub>): δ 7.92 (td,

 $^{3}J_{\mathrm{H-H}} = 7.5$ ,  $^{5}J_{\mathrm{P-H}} = 1.8$  Hz, 4H), 7.80 (td,  $^{3}J_{\mathrm{H-H}} = 7.8$ ,  $^{4}J_{\mathrm{P-H}} = 3.4$  Hz, 8H), 7.70–7.55 (m, 8H), 1.92 (s, 3H).  $^{13}\mathrm{C}\{^{1}\mathrm{H}\}$  NMR (126 MHz, CDCl<sub>3</sub>):  $\delta$  176.5, 135.9 (d,  $^{4}J_{\mathrm{P-C}} = 3.1$  Hz), 134.4 (d,  $^{3}J_{\mathrm{P-C}} = 10.4$  Hz), 130.8 (d,  $^{2}J_{\mathrm{P-C}} = 12.8$  Hz), 117.4 (d,  $^{1}J_{\mathrm{P-C}} = 89.5$  Hz) 25.6.  $^{31}\mathrm{P}\{^{1}\mathrm{H}\}$  NMR (203 MHz, CDCl<sub>3</sub>):  $\delta$  23.1. IR-ATR 3167, 3050, 1592, 1435, 1371, 1107, 995, 723, 692 cm<sup>-1</sup>. HRMS-ESI calcd for  $\mathrm{C}_{24}\mathrm{H}_{20}\mathrm{P}$  (M – OAc)<sup>+</sup>, 339.1298; found, 339.1315.

*Bis*(*triphenylphosphine*)*iminium Acetate* (*5OAc*). Bis(triphenylphosphine)*iminium* chloride (250 mg, 0.44 mmol, 1.0 equiv) dissolved in 1:1 methanol/water afforded 247 mg (95%) of the acetate salt as a white solid via the general procedure. This powder was dried under vacuum (<0.1 Torr) for 24 h at room temperature (mp 118–120 °C).  $^{1}$ H NMR (400 MHz, CDCl<sub>3</sub>): δ 7.70–7.66 (m, 6H), 7.51–7.42 (m, 24H), 1.98 (s, 3H).  $^{13}$ C{ $^{1}$ H} NMR (126 MHz, CDCl<sub>3</sub>): δ 177.1, 134.0, 132.7–131.3 (m), 130.5–128.8 (m), 127.0 (dd, J = 108.0 and 2.0 Hz), 25.2.  $^{31}$ P{ $^{1}$ H} NMR (162 MHz, CDCl<sub>3</sub>): δ 21.1. IR-ATR 3055, 1567, 1440, 1385, 1265, 1115 cm $^{-1}$ . HRMS-ESI calcd for  $C_{36}$ H<sub>30</sub>NP<sub>2</sub> (M – OAc) $^{+}$ , 538.1848; found, 538.1876.

*P2 Acetate* (4OAc). P2 tetrafluoroborate (350 mg, 0.82 mmol, 1.0 equiv) afforded the acetate salt as a clear oil. After removing some of the remaining water via azeotropic distillation with benzene on a rotary evaporator, the clear wax was dried at <0.1 Torr for 48 h at room temperature to afford 305 mg (93%) of the product as a white solid (mp 177–180 °C). <sup>1</sup>H NMR (400 MHz, CDCl<sub>3</sub>): δ 2.68 (t,  $J_{\rm N-H} = 5.3$  Hz, 36H), 1.98 (s, 3H). <sup>13</sup>C{<sup>1</sup>H} NMR (126 MHz, CDCl<sub>3</sub>): δ 176.1, 36.7, 24.0. <sup>31</sup>P{<sup>1</sup>H} NMR (203 MHz, CDCl<sub>3</sub>): δ 16.8. IR-ATR 2896, 2851, 2807, 1586, 1466, 1365, 1297, 1177, 974, 742 cm<sup>-1</sup>. HRMS-ESI calcd for C<sub>12</sub>H<sub>36</sub>N<sub>7</sub>P<sub>2</sub> (M – OAc)<sup>+</sup>, 340.2502; found, 340.2508.

*P5 Acetate* (*6OAc*). P5 chloride (200 mg, 0.26 mmol) afforded the acetate salt as a clear oil that was soluble in benzene. After azeotropically distilling off excess water on a rotary evaporator, the waxy solid was dried under vacuum (<0.01 Torr) in a nitrogen glovebox at 60 °C to afford 185 mg (90%) of a pale-blue solid (mp not determined; the compound is deliquescent). <sup>1</sup>H NMR (500 MHz, CDCl<sub>3</sub>): δ 2.61 (d,  $J_{P-H}$  = 9.9 Hz, 72H), 2.04 (s, 3H). <sup>13</sup>C{<sup>1</sup>H} NMR (126 MHz, CDCl<sub>3</sub>): δ 173.6, 37.0 (d,  $J_{P-C}$  = 5.0 Hz), 23.1. <sup>31</sup>P{<sup>1</sup>H} NMR (203 MHz, CDCl<sub>3</sub>): δ 6.1 (d, J = 55 Hz), -34.9 (t, J = 55 Hz). IR-ATR 2999, 2892, 2802, 1651, 1580, 1462, 1292, 1195, 985, 736 cm<sup>-1</sup>. HRMS-ESI calcd for  $C_{24}H_{72}N_{16}P_5$  (M - OAc)<sup>+</sup>, 739.4809; found, 739.4795.

General Procedure for the Synthesis of Chloride Salts. The synthesis of the chloride salts was accomplished in an identical manner to the acetates using Dowex Marathon A2 or AmberLite IRA67 weakly basic resin in their chloride forms  $(2 \times 40 \text{ cm column}, \gg 10 \text{ equiv})$ .

*P2 Chloride (4Cl)*. The P2 tetrafluoroborate salt (1.01 g, 2.36 mmol, 1.0 equiv) afforded 844 mg (95%) of the corresponding chloride as a white solid using the general procedure with Dowex Marathon A2 resin (mp > 240 °C).  $^{1}$ H NMR (400 MHz, CDCl<sub>3</sub>): δ 2.60 (t,  $J_{\rm N-H}$  = 5.1 Hz, 36H).  $^{13}$ C{ $^{1}$ H} NMR (101 MHz, CDCl<sub>3</sub>): δ 36.7 (t,  $J_{\rm N-C}$  = 2.4 Hz).  $^{31}$ P{ $^{1}$ H} NMR (162 MHz, CDCl<sub>3</sub>): δ 16.8. IR-ATR 2987, 2905, 2852, 2810, 1492, 1470, 1388, 1302, 1184, 1068, 986, 746 cm $^{-1}$ . HRMS-ESI calcd for  $C_{12}$ H<sub>36</sub>N<sub>7</sub>P<sub>2</sub> (M - Cl) $^{+}$ , 340.2502; found, 340.2515.

General Procedure for the Synthesis of Phosphonium Chlorides. A 50 mL two-necked round-bottomed flask equipped with an addition funnel and a rubber septum was purged with argon. Freshly burnished magnesium turnings (4 equiv) and THF (15 mL or 0.67 M with respect to the aryl bromide) were added, the flask was heated to 35 °C, and four drops of dibromoethane were added as an initiator. The corresponding aryl bromide (3.5 equiv) was dissolved in THF (15 mL or 0.67 M with respect to the aryl bromide) and added dropwise via the addition funnel over 30 min. The resulting solution was stirred for 3 h and then cooled to 0 °C. An approx. 2 M solution containing 1 equiv of PCl<sub>3</sub> in DCM was prepared and added dropwise over 2 h using a syringe pump. The reaction mixture was slowly allowed to warm to room temperature and stirred overnight. Water was subsequently added, followed by 50 mL of DCM, and the organic layer was washed twice with water (50 mL portions) and once with

brine (50 mL). It was then dried with  $MgSO_4$ , the solvent was removed using a rotary evaporator, and the intermediate phosphine was purified via medium-pressure liquid chromatography (MPLC); see the specific procedures for the solvents used. The resulting waxy white or pale-yellow solid was dried for 24 h under vacuum (<0.1 Torr) at room temperature.

The phosphine's purity was checked by 31P and 1H NMR to confirm that the phosphine oxide was only minimally present, and then it was added to a pressure tube equipped with an air-free sidearm. A selected aryl bromide (1.0 equiv) was added along with 3 mL (approx. 0.5 M) of degassed m-xylene, and this solution was degassed via three freeze-pump-thaw cycles. The tube was then opened, Pd<sub>2</sub>(dba)<sub>3</sub> (0.05 equiv) was added, the resulting mixture was degassed an additional two times, and the pressure tube was filled with argon as it was warmed to room temperature. The sealed vessel was placed in an oil bath at 145 °C and stirred for 18 h, after which 75 mL of Et<sub>2</sub>O was added, and the resulting slurry was stirred for 1 h. It was then poured onto a 1 in. silica plug in a Buchner funnel with a medium-porosity glass frit and washed with 200 mL of Et<sub>2</sub>O, and phosphonium bromide was eluted using one of several solvents as specified for the specific compounds. Concentration of the eluent afforded the phosphonium bromide, which was converted to the chloride salt without further purification using the general procedure in water/methanol (1:1) with an IRA-67 chloride ion exchange

*Tetrakis*(*4-methylphenyl*)*phosphonium Chloride* (*8CI*). The commercially available tris(4-methylphenyl)phosphine (512 mg, 1.68 mmol, 1.0 equiv) afforded 270 mg (34%) of the recrystallized phosphonium bromide according to the general procedure with 100 mL of DCM used as the eluent for the silica plug and ethanol for recrystallization. A portion of the bromide salt (141 mg, 0.30 mmol) was converted to 121 mg (95%) of the chloride salt, which needed no further purification (mp > 240 °C). IR-ATR 3015, 2973, 2923, 1637, 1596, 1446, 1401, 1316, 1192, 1107, 811, 664 cm<sup>-1</sup>. <sup>1</sup>H NMR (500 MHz, CDCl<sub>3</sub>): δ 7.52 (dd,  $^{3}J_{\rm H-H}$  = 8.2 Hz,  $^{4}J_{\rm P-H}$  = 3.3 Hz, 8H), 7.42 (dd,  $^{3}J_{\rm H-H}$  = 8.0 Hz,  $^{4}J_{\rm P-H}$  = 12.7 Hz, 8H), 2.51 (s, 12H).  $^{13}$ C{<sup>1</sup>H} NMR (101 MHz, CDCl<sub>3</sub>): δ 147.0 (d,  $J_{\rm P-C}$  = 3.0 Hz), 134.0 (d, J = 10.7 Hz), 131.3 (d, J = 13.4 Hz), 114.6 (d, J = 92.5 Hz), 21.8 (d, J = 1.6 Hz).  $^{31}$ P{<sup>1</sup>H} NMR (203 MHz, CDCl<sub>3</sub>): δ 22.1. HRMS-ESI calcd for  $C_{28}H_{28}$ P (M − Cl)<sup>+</sup>, 395.1924; found, 395.1933.

Tetrakis(4-t-butylphenyl)phosphonium Chloride (9CI). The general procedure using 1-bromo-4-t-butylbenzene (2.13 g, 10.0 mmol, 3.5 equiv), magnesium turnings (277 mg, 11.4 mmol, 4.0 equiv), and PCl<sub>3</sub> (343 mg, 2.86 mmol, 1.0 equiv) afforded 568 mg (1.32 mmol, 46%) of the triarylphosphine [ $^{31}$ P NMR (162 MHz, CDCl<sub>3</sub>):  $\delta$ -8.91]. It was purified by MPLC using 10% EtOAc in hexanes, dried, concentrated with a rotary evaporator, and converted via the general procedure to 313 mg (36%) of the phosphonium bromide. A portion of this material (150 mg, 0.23 mmol) was boiled in water for 15 min and hot-filtered to remove insoluble impurities, then H2O was removed under vacuum, and the residue was converted to 130 mg (96%) of the chloride salt (mp > 240 °C). IR-ATR 3061, 2960, 2908, 2868, 1596, 1394, 1091, 830, 759, 639 cm<sup>-1</sup>. <sup>1</sup>H NMR (500 MHz, CDCl<sub>3</sub>):  $\delta$  7.73 (dd,  ${}^{3}J_{H-H}$  = 8.5 Hz,  ${}^{4}J_{P-H}$  = 3.2 Hz, 8H), 7.51 (dd,  ${}^{3}J_{H-H}$  = 8.5 Hz,  ${}^{4}J_{P-H}$  = 12.7 Hz, 8H), 1.36 (s, 36H).  ${}^{13}C\{{}^{1}H\}$  NMR (126 MHz, CDCl<sub>3</sub>):  $\delta$  159.7 (d,  ${}^{4}J_{P-C}$  = 3.1 Hz), 134.1 (d,  ${}^{3}J_{P-C}$  = 10.6 Hz), 127.6 (d,  ${}^{2}J_{P-C}$  = 13.1 Hz), 114.6 (d,  ${}^{1}J_{P-C}$  = 92.3 Hz), 35.5, 30.8.  $^{31}P\{^{1}H\}$  NMR (203 MHz, CDCl<sub>3</sub>):  $\delta$  21.0. HRMS-ESI calcd for  $C_{40}H_{52}P$  (M – Cl)+, 563.3802; found, 563.3816.

Tetrakis(3,5-dimethylphenyl)phosphonium Chloride (10Cl). The general procedure using 1-bromo-3,5-dimethylbenzene (1.50 g, 8.11 mmol, 3.5 equiv), magnesium turnings (225 mg, 9.27 mmol, 4.0 equiv), and PCl<sub>3</sub> (319 mg, 2.32 mmol, 1.0 equiv) afforded 730 mg (2.11 mmol, 91%) of the corresponding phosphine ( $^{31}$ P (162 MHz, CDCl<sub>3</sub>):  $\delta$  –4.72). It was purified by MPLC using 20% EtOAc in hexanes and converted to 360 mg (32%) of the phosphonium bromide via the general procedure. The silica plug was washed first with 150 mL of Et<sub>2</sub>O and then with 150 mL of DCM, and the phosphonium salt was eluted with 50% methanol in DCM. A portion of this material (250 mg, 0.47 mmol) afforded 225 mg (98%) of the

chloride salt (mp > 240 °C). IR-ATR 3187, 2981, 2945, 2921, 1593, 1455, 1268, 1128, 1033, 872, 848, 686 cm $^{-1}$ .  $^{1}$ H NMR (400 MHz, CDCl $_3$ ):  $\delta$  7.47 (d,  $^{4}J_{\rm H-H}$  = 2.1 Hz, 4H), 7.07 (dd,  $^{3}J_{\rm P-H}$  = 13.3 Hz,  $^{1}J_{\rm H-H}$  = 1.6 Hz, 8H), 2.41 (s, 24H).  $^{13}{\rm C}\{^{1}{\rm H}\}$  NMR (101 MHz, CDCl $_3$ ):  $\delta$  140.6 (d,  $^{1}J_{\rm P-C}$  = 13.6 Hz), 137.3 (d,  $^{2}J_{\rm P-C}$  = 3.2 Hz), 131.6 (d,  $^{3}J_{\rm P-C}$  = 10.2 Hz), 117.7 (d,  $^{4}J_{\rm P-C}$  = 88.3 Hz), 21.6.  $^{31}{\rm P}\{^{1}{\rm H}\}$  NMR (162 MHz, CDCl $_3$ ):  $\delta$  22.8. HRMS-ESI calcd for C $_{32}$ H $_{36}$ P (M $_{\rm C}$ Cl) $^{4}$ , 451.2550; found, 451.2559.

Tetrakis(4-N,N-dimethylaminophenyl)phosphonium Chloride (11CI). The general procedure with 4-bromo-N,N-dimethylaminobenzene (4.00 g, 20.0 mmol, 3.5 equiv), magnesium turnings (557 mg, 22.9 mmol, 4.0 equiv), and PCl<sub>3</sub> (784 mg, 5.71 mmol, 1.0 equiv) afforded 1.76 g (4.50 mmol, 79%) of the triarylphosphine (31P NMR (162 MHz, CDCl<sub>3</sub>):  $\delta$  –11.2). It was purified by MPLC starting with 10% EtOAc in hexanes, ramped up to 100% EtOAc, and concentrated under vacuum, and 1.66 g (4.24 mmol) was converted to 1.35 g (54%) of phosphonium bromide using the general procedure. In this case, the silica plug was washed first with 150 mL of ether and then with 75 mL of DCM before the bromide salt was eluted with 250 mL of a 1:1 THF/DCM mixture. A portion of this material (550 mg, 0.93 mmol) was recrystallized in hot water with hot filtration to remove insoluble impurities prior to conversion to 483 mg (95%) of the phosphonium chloride (mp > 240 °C). IR-ATR 3190, 3033, 2923, 2824, 1596, 1524, 1445, 1378, 1296, 1230, 1210, 1109, 814, 772, 649 cm<sup>-1</sup>.  $^{1}$ H NMR (500 MHz, CDCl<sub>3</sub>):  $\delta$  7.28 (dd,  $^{3}J_{P-H}$  = 11.7 Hz,  ${}^{3}J_{H-H}$  8.8 Hz, 8H), 6.78 (dd,  ${}^{3}J_{H-H}$  = 9.0 Hz,  ${}^{4}J_{P-H}$  2.6 Hz, 8H), 3.08 (s, 24H).  $^{13}C\{^{1}H\}$  NMR (101 MHz, CDCl<sub>3</sub>):  $\delta$  153.4 (d,  $^{4}J_{P-C}$  = 2.3 Hz), 135.0 (d,  ${}^{3}J_{P-C}$  = 11.5 Hz), 112.0 (d,  ${}^{2}J_{P-C}$  = 13.5 Hz), 103.6 (d,  $^{1}J_{P-C}$  = 103.8 Hz), 39.9.  $^{31}P\{^{1}H\}$  NMR (203 MHz, CDCl<sub>3</sub>):  $\delta$  18.8. HRMS-ESI calcd for C<sub>32</sub>H<sub>40</sub>N<sub>4</sub>P (M - Cl)<sup>+</sup>, 511.2986; found, 511.3013.

Tetrakis(3,5-dimethoxyphenyl)phosphonium Chloride (12CI). The general procedure with 1-bromo-3,5-dimethoxybenzene (4.34 g, 20.0 mmol, 3.5 equiv), magnesium turnings (557 mg 22.4 mmol, 4.0 equiv), and PCl<sub>3</sub> (784 mg, 5.70 mmol, 1.0 equiv) afforded 2.03 g (4.59 mmol, 81%) of the phosphine ( $^{31}$ P NMR ( $^{162}$  MHz, CDCl $_{3}$ ):  $\delta$ 0.87). It was purified via MPLC starting with 10% EtOAc in hexanes, ramped up to 100% EtOAc, and concentrated under vacuum, and all of it was converted to 1.68 g (55%) of phosphonium bromide using the general procedure. In this case, the silica plug was washed with 75 mL of DCM in addition to the ether wash, and the bromide salt was eluted with 250 mL of a 1:1 THF/DCM mixture. A portion of this material (504 mg, 0.76 mmol) was recrystallized in hot water with hot filtration to remove insoluble impurities prior to conversion to 423 mg (90%) of phosphonium chloride (mp 222-225 °C). IR-ATR 3076, 3011, 2981, 2943, 2843, 1585, 1455, 1423, 1309, 1295, 1207, 1165, 1065, 1035, 869, 843 cm<sup>-1</sup>.  $^{1}$ H NMR (400 MHz, CDCl<sub>3</sub>):  $\delta$ 6.91 (s, 4H), 6.63 (d, I = 14.4 Hz, 8H), 3.86 (s, 24H).  ${}^{13}C{}^{1}H$  NMR (126 MHz, CDCl<sub>3</sub>):  $\delta$  162.2 (d, J = 19.7 Hz), 118.7 (d, J = 90.3 Hz), 112.6 (d, J = 11.6 Hz), 105.8, 56.2  $^{31}P\{^{1}H\}$  NMR (162 MHz, CDCl<sub>3</sub>):  $\delta$  26.5. HRMS-ESI calcd for C<sub>32</sub>H<sub>36</sub>O<sub>8</sub>P (M - Cl)<sup>+</sup>, 579.2143; found, 579.2167.

*P4-t-Bu-HCl* (*13Cl*). A P4-*t*-Bu base solution ( $\sim$ 0.8 M in THF, 1 equiv) was diluted with 15 mL of freshly distilled THF. In a separate two-necked round-bottomed flask, 10 mL of concentrated HCl was added slowly to a bed of anhydrous calcium chloride pellets. The resulting gaseous HCl was transferred to the reaction flask with argon as a carrier gas and bubbled through the solution for 30 min. The reaction mixture was concentrated and dried under vacuum (<0.1 Torr) to afford the HCl salt of P4-*t*-Bu without further purification (mp 82–84 °C). IR-ATR 2930, 2811, 2457, 1632, 1562, 1464, 1377, 1296, 1187, 1067, 989, 751 cm<sup>-1</sup>. <sup>1</sup>H NMR (500 MHz, CDCl<sub>3</sub>): δ 9.79 (s, 1H), 2.77 (d,  $^{3}J_{P-H} = 10.3$  Hz, 54H), 1.45 (s, 9H).  $^{13}C\{^{1}H\}$  NMR (126 MHz, CDCl<sub>3</sub>): δ 37.5 (d,  $^{2}J_{P-C} = 4.9$  Hz), 34.9, 30.9.  $^{31}P\{^{1}H\}$  NMR (162 MHz, DMSO): δ 12.7 (d, J = 48.5 Hz) -23.6 (br s). HRMS-ESI calcd for  $C_{22}H_{64}N_{13}P_{4}$  (M - Cl)  $^{+}$  634.4353; found, 634.4333

General Procedure for the Synthesis of Tetrafluoroborate Salts. To a 25 mL round-bottomed flask, the corresponding chloride or bromide salt (1 equiv) was dissolved in acetone/DCM (1:1).

Excess sodium tetrafluoroborate (3+ equiv) was added, and the mixture was vigorously stirred overnight. The insoluble salts were filtered off, and the filtrate was concentrated. The resultant solid was redissolved in DCM and filtered once more. Removal of the solvent on a rotary evaporator afforded the tetrafluoroborate salt.  $^{19}F\{^1H\}$  NMR were collected at a concentration of 50 mM with 10 mM fluorobenzene as an internal standard referenced to -113.90.  $^{78}$ 

Tetraphenylphosphonium Tetrafluoroborate (7BF<sub>4</sub>). The general procedure with tetraphenylphosphonium chloride (50 mg, 0.13 mmol, 1.0 equiv) afforded 53 mg (93%) of the known tetrafluoroborate salt. <sup>82</sup> <sup>1</sup>H NMR (400 MHz, CD<sub>2</sub>Cl<sub>2</sub>):  $\delta$  8.14–7.84 (m, 4H), 7.88–7.71 (m, 8H), 7.72–7.48 (m, 8H)). <sup>19</sup>F{<sup>1</sup>H} NMR (376 MHz, CD<sub>2</sub>Cl<sub>2</sub>):  $\delta$  –153.34.

Bis(triphenylphosphine)iminium Tetrafluoroborate (5BF<sub>4</sub>). The general procedure with PPN chloride (50 mg, 0.87 mmol, 1.0 equiv) afforded 53 mg (98%) of the known tetrafluoroborate salt. <sup>83</sup> <sup>1</sup>H NMR (400 MHz, CD<sub>2</sub>Cl<sub>2</sub>):  $\delta$  8.31–7.62 (m, 6H), 7.60–6.29 (m, 24H). <sup>19</sup>F{<sup>1</sup>H} NMR (376 MHz, CD<sub>2</sub>Cl<sub>2</sub>):  $\delta$  –153.44.

Tetrakis[tris(dimethylamino)phosphoranylidenamino]-phosphonium Tetrafluoroborate (4BF<sub>4</sub>). The title compound was synthesized by a previous group member using the procedure reported by Link and Schwesinger. <sup>48,84</sup> <sup>1</sup>H NMR (500 MHz, CDCl<sub>3</sub>):  $\delta$  2.67 (t,  ${}^2J_{\rm N-H}$  = 5.3 Hz, 36H). <sup>19</sup>F{ $^1$ H} NMR (376 MHz, CD<sub>2</sub>Cl<sub>2</sub>):  $\delta$  –153.41.

Tetrakis[tris(dimethylamino)phosphoranylidenamino]-phosphonium Tetrafluoroborate (6BF<sub>4</sub>). The general procedure using P5 chloride (50 mg, 0.64 mmol, 1.0 equiv) afforded the tetrafluoroborate salt in quantitative yield (53 mg, 100%). The resulting spectra are in agreement with those in previous reports. <sup>83</sup> <sup>1</sup>H NMR (500 MHz, CDCl<sub>3</sub>): δ 2.62 (d,  $^3J_{P-H}$  = 9.8 Hz, 72H).  $^{19}F\{^1H\}$  NMR (376 MHz, CD<sub>2</sub>Cl<sub>2</sub>): δ -153.47.

*Tetrakis*(*4*-methylphenyl)phosphonium Tetrafluoroborate (*8BF*<sub>4</sub>). The general procedure with the appropriate phosphonium bromide (200 mg, 0.42 mmol, 1.0 equiv) afforded 198 mg (98%) of the tetrafluoroborate salt as an off-white solid (mp 239–241 °C). IR-ATR 3031, 2957, 2923, 2869, 1598, 1499, 1402, 1108, 1059, 807, 663 cm<sup>-1</sup>. <sup>1</sup>H NMR (400 MHz, CDCl<sub>3</sub>): δ 7.52 (dd, <sup>3</sup> $J_{\text{H-H}}$  = 8.3, <sup>4</sup> $J_{\text{P-H}}$  = 3.4 Hz, 8H), 7.45 (dd, <sup>3</sup> $J_{\text{P-H}}$  = 12.6, <sup>3</sup> $J_{\text{H-H}}$  = 8.3 Hz, 8H), 2.51 (s, 12H). <sup>13</sup>C{<sup>1</sup>H} NMR (101 MHz, CDCl<sub>3</sub>): δ 147.0 (d, <sup>4</sup> $J_{\text{P-C}}$  = 3.1 Hz), 134.0 (d, <sup>3</sup> $J_{\text{P-C}}$  = 10.7 Hz), 131.3 (d, <sup>2</sup> $J_{\text{P-C}}$  = 13.4 Hz), 114.6 (d, <sup>1</sup> $J_{\text{P-C}}$  = 92.8 Hz), 21.8 (d, <sup>5</sup> $J_{\text{P-C}}$  = 1.6 Hz). <sup>19</sup>F{<sup>1</sup>H} NMR (376 MHz, CD<sub>2</sub>Cl<sub>2</sub>): δ −153.39. <sup>31</sup>P{<sup>1</sup>H} NMR (162 MHz, CDCl<sub>3</sub>): δ 22.1. HRMS-ESI calcd for C<sub>28</sub>H<sub>28</sub>P (M − BF<sub>4</sub>)<sup>+</sup>, 395.1924; found, 395.1950.

*Tetrakis*(4-t-butylphenyl)phosphonium *Tetrafluoroborate* (*9BF*<sub>4</sub>). The general procedure with the requisite phosphonium bromide (150 mg, 0.23 mmol, 1.0 equiv) afforded 150 mg (99%) of the tetrafluoroborate salt as a bright-yellow—orange solid (mp > 240 °C). IR-ATR 2964, 2907, 2870, 1596, 1396, 1092, 1055, 829, 759, 639 cm<sup>-1</sup>. <sup>1</sup>H NMR (400 MHz, CDCl<sub>3</sub>): δ 7.75 (dd, <sup>3</sup>*J*<sub>H−H</sub> = 8.4 Hz, <sup>4</sup>*J*<sub>P−H</sub> = 3.2 Hz, 8H), 7.54 (dd, <sup>3</sup>*J*<sub>P−H</sub> = 12.6 Hz, <sup>3</sup>*J*<sub>H−H</sub> = 8.2 Hz, 8H), 1.38 (s, 36H). <sup>13</sup>C{<sup>1</sup>H} NMR (126 MHz, CDCl<sub>3</sub>): δ 159.5 (d, <sup>4</sup>*J*<sub>P−C</sub> = 2.9 Hz), 134.1 (d, <sup>3</sup>*J*<sub>P−C</sub> = 10.8 Hz), 127.6 (d, <sup>2</sup>*J*<sub>P−C</sub> = 13.1 Hz), 114.6 (d, <sup>1</sup>*J*<sub>P−C</sub> = 92.4 Hz), 35.5, 30.8. <sup>19</sup>F{<sup>1</sup>H} NMR (376 MHz, CD<sub>2</sub>Cl<sub>2</sub>): δ −153.48. <sup>31</sup>P{<sup>1</sup>H} NMR (162 MHz, CDCl<sub>3</sub>): δ 20.9. HRMS-ESI calcd for C<sub>40</sub>H<sub>52</sub>P (M − BF<sub>4</sub>)<sup>+</sup>, 563.3802; found, 563.3835.

*Tetrakis*(3,5-dimethylphenyl)phosphonium Tetrafluoroborate (10BF<sub>4</sub>). The general procedure with the corresponding phosphonium bromide (328 mg, 0.62 mmol, 1.0 equiv) afforded 316 mg (95%) of the tetrafluoroborate salt as a yellow solid (mp 215–219 °C with decomp). IR-ATR 2955, 2919, 1598, 1450, 1268, 1127, 1097, 1057, 853, 684 cm<sup>-1</sup>. <sup>1</sup>H NMR (500 MHz, CDCl<sub>3</sub>): δ 7.48 (s, 4H), 7.10 (d,  $^3J_{\rm P-H}$  = 13.3 Hz, 8H), 2.42 (s, 24H).  $^{13}$ C{ $^1$ H} NMR (126 MHz, CDCl<sub>3</sub>): δ 140.6 (d,  $^2J_{\rm P-C}$  = 13.4 Hz), 137.3 (d,  $^4J_{\rm P-C}$  = 3.3 Hz), 131.6 (d,  $^3J_{\rm P-C}$  = 10.0 Hz), 117.7 (d,  $^1J_{\rm P-C}$  = 88.3 Hz), 21.5.  $^{19}$ F{ $^1$ H} NMR (376 MHz, CD<sub>2</sub>Cl<sub>2</sub>): δ −153.45.  $^{31}$ P{ $^1$ H} NMR (203 MHz, CDCl<sub>3</sub>): δ 22.8. HRMS-ESI calcd for C<sub>32</sub>H<sub>36</sub>P (M − BF<sub>4</sub>)<sup>+</sup>, 451.2550; found, 451.2572.

Tetrakis(4-dimethylaminophenyl)phosphonium Tetrafluoroborate (11BF<sub>4</sub>). The general procedure with the appropriate

phosphonium bromide (120 mg, 0.20 mmol, 1.0 equiv) afforded 112 mg (93%) of the tetrafluoroborate salt as a pale-brown solid (mp > 240 °C). IR-ATR 2919, 2161, 2026, 1594, 1520, 1375, 1107, 1064 cm<sup>-1</sup>. <sup>1</sup>H NMR (500 MHz, CDCl<sub>3</sub>): δ 7.28 (dd,  ${}^{3}J_{P-H} = 11.9$  Hz,  ${}^{3}J_{H-H} = 9.0$  Hz, 8H), 6.78 (dd,  ${}^{3}J_{H-H} = 9.1$ ,  ${}^{4}J_{P-H} = 2.6$  Hz, 8H), 3.08 (s, 24H).  ${}^{13}C\{{}^{1}H\}$  NMR (126 MHz, CDCl<sub>3</sub>): δ 153.4 (d,  ${}^{4}J_{P-C} = 2.4$  Hz), 135.0 (d,  ${}^{3}J_{P-C} = 11.7$  Hz), 112.0 (d,  ${}^{2}J_{P-C} = 13.5$  Hz), 103.6 (d,  ${}^{1}J_{P-C} = 103.6$  Hz), 39.9.  ${}^{19}F\{{}^{1}H\}$  NMR (376 MHz, CD<sub>2</sub>Cl<sub>2</sub>): δ –153.50.  ${}^{31}P\{{}^{1}H\}$  NMR (203 MHz, CDCl<sub>3</sub>): δ 18.8. HRMS-ESI calcd for C<sub>32</sub>H<sub>40</sub>N<sub>4</sub>P (M – BF<sub>4</sub>)<sup>+</sup>, 511.2986; found, 511.3008.

Tetrakis(3,5-dimethoxyphenyl)phosphonium Tetrafluoroborate (12BF<sub>4</sub>). The general procedure with the needed phosphonium bromide (101 mg, 0.15 mmol, 1.0 equiv) afforded 94 mg (92%) of the tetrafluoroborate salt (mp ~ 242 °C with decomp). IR-ATR 3081, 3009, 2942, 2842, 1584, 1456, 1422, 1310, 1295, 1209, 1166, 1066, 1036, 869, 845, 824, 684 cm<sup>-1</sup>. <sup>1</sup>H NMR (400 MHz, CDCl<sub>3</sub>): δ 6.90 (t, <sup>4</sup>J<sub>H-H</sub> = 2.2 Hz, 4H), 6.64 (dd, <sup>3</sup>J<sub>P-H</sub> = 14.4 Hz, <sup>4</sup>J<sub>H-H</sub> = 2.2 Hz, 8H), 3.86 (s, 24H). <sup>13</sup>C{<sup>1</sup>H} NMR (126 MHz, CDCl<sub>3</sub>): δ 162.2 (d, <sup>2</sup>J<sub>P-C</sub> = 19.6 Hz), 118.7 (d, <sup>1</sup>J<sub>P-C</sub> = 90.4 Hz), 112.6 (d, <sup>3</sup>J<sub>P-C</sub> = 11.7 Hz), 105.8, 56.1. <sup>19</sup>F{<sup>1</sup>H} NMR (376 MHz, CD<sub>2</sub>Cl<sub>2</sub>): δ −153.38. <sup>31</sup>P{<sup>1</sup>H} NMR (162 MHz, CDCl<sub>3</sub>): δ 26.5. HRMS-ESI calcd for C<sub>32</sub>H<sub>36</sub>O<sub>8</sub>P (M − BF<sub>4</sub>)<sup>+</sup>, 579.2143; found, 579.2133.

IR Procedure. A solution of the chloride salt of interest was prepared in  $CDCl_3$  at a concentration of 50 mM. A spectrum was taken using a liquid IR cell with a 0.1 mm path length and NaCl windows. The difference between the unbound C–D stretch (2253 cm<sup>-1</sup>) and the bound C–D stretch (~2190 cm<sup>-1</sup>) was recorded.

General Procedure for Acetate Kinetics. A second-order  $\rm S_{\rm N}2$  reaction was performed with target concentrations of 100 mM for the acetate salt and 75 mM for 1-iodooctane. The salts were weighed out in vials in a nitrogen glovebox, and CDCl $_{\rm 3}$  solutions containing the appropriate amount of the iodide were added to them outside of the glovebox. The contents were thoroughly mixed and then transferred to an NMR tube that was sealed with electrical tape in addition to the NMR cap to limit solvent evaporation.  $^{\rm 1}{\rm H}$  NMR spectra were recorded at periodic intervals and used to determine reaction conversions by comparing the methylene triplets of the starting material and product at 3.14 and 4.00 ppm, respectively; no evidence for the formation of 1-octene was observed.

*P4-t-Bu·H*<sup>+</sup> Acetate Kinetics. An argon-purged flask was charged with 0.47 mL (0.063 mmol) of 0.8 M P4-t-Bu in hexane, and this solution was diluted with 5 mL of freshly distilled THF. Acetic acid dried over CuSO<sub>4</sub> (1.0 equiv) was dissolved in 2 mL of THF and then added to the P4-t-Bu base. This mixture was concentrated and dried for 24 h at 25 °C under vacuum with a mechanical pump to give the acetate salt in a quantitative yield. It was immediately used in kinetic runs without further purification.

General Procedure for Chloride Kinetics. Pseudo-first-order S<sub>N</sub>2 reactions were performed with 25 and 250 mM concentrations of the chloride salt and 1-iodooctane, respectively. The former compounds were directly weighted into quartz cuvettes in a nitrogen glovebox, and subsequently, CH2Cl2 solutions of 1-iodooctane were added through the attached (and electrically taped) Mininert valve. The resulting reaction mixtures were thoroughly shaken before being placed into the UV-vis instrument at 25.0 °C. All runs for each compound were monitored simultaneously and set up sequentially, so the t = 0 point for each run varies slightly due to the 2–5 min it takes to prepare the solutions. As a result, the observed and calculated  $A_0$ values vary, but this has no effect on the results since the kinetics were performed under pseudo-first-order conditions. Reaction progress was monitored at 367 nm for the appearance of the corresponding iodide salt in all cases except for the tetrakis(3,5-dimethoxyphenyl)phosphonium cation where this wavelength corresponded to the disappearance of the starting chloride salt. NMR spectroscopy was used to confirm the reliability of the UV-vis data in the case of the (3,5-Me<sub>2</sub>C<sub>6</sub>H<sub>3</sub>)<sub>4</sub>P chloride due to the sinusoidal behavior observed in the UV kinetic trace. NMR was also used to monitor the reaction with the P5 chloride since a calibration curve revealed a nonlinear relationship between absorbance and the concentration of its iodide salt. A linear pseudo-first-order fit of the data was used for the NMR

data. Nonlinear least-square fits were carried out for the UV—vis data using Excel by minimizing the sums of the squared errors between the calculated and the observed results for eq 6, where k,  $A_0$ , and  $A_{\inf}$  were treated as variables.

$$A_t = A_{\text{inf}} - (A_{\text{inf}} - A_0)e^{-kt}$$
 (6)

NMR data for  $(3,5\text{-Me}_2C_6H_3)_4P$ , PPN, and P5 chlorides were individually obtained by weighing each compound in a nitrogen glovebox and dissolving it in a solution of 250 mM 1-iodooctane in  $\text{CD}_2\text{Cl}_2$  or  $\text{CD}_3\text{CN}$  so that the concentration of the chloride salt was 25 mM. The reaction mixtures were then transferred to NMR tubes and placed inside a 400 or 500 MHz spectrometer and held at 25.0 °C. Linear least-square plots of  $\ln[\text{MCl}]$  versus time led to the observed rate constants.

General Procedure for NMR Titrations. To a 1 mL volumetric flask in a nitrogen glovebox, the appropriate mass of chloride salt was added to afford the desired stock solution concentration. The flask was sealed and removed from the glovebox, at which point the solution was prepared. A small aliquot  $(5-20~\mu\text{L})$  of the stock solution was added to another 1 mL vol. flask and diluted to give the starting concentration. In the case of TBA, an intermediate  $10\times$  dilution was prepared to give a sufficiently low starting concentration. The entire starting solution was transferred to an argon-purged screw top NMR tube equipped with a cap with a PTFE-lined septum and transferred to the instrument. Aliquots of the stock solution were added using gas-tight microsyringes, the tube was inverted six times to facilitate mixing, and the shifts and concentrations were fitted with the BindFit app's dimerization model  $^{51,74}$  to give the reported  $K_{\rm ip}$  values.

Catalytic Experiments. A 2-dram vial was charged with tetramethylammonium acetate (20.3 mg, 150 mmol), a catalytic amount of the selected chloride salt (10 mol %), and a 1 cm stir bar. A 50 mM solution of 1-iodooctane (2 mL, 100 mmol) in either DCM/Et<sub>2</sub>O (1:1) or DCM was added and the vial was placed into a heating block at 30 °C. Stirring was performed at 360 rpm throughout the reaction, and after 2.5 h, the vial was filled with water and shaken vigorously to remove the unreacted acetate salt and halt the reaction progress. The organic layer was pipetted off, dried with MgSO<sub>4</sub>, and concentrated under reduced pressure. Chloroform-*d* was added to the residue to obtain a <sup>1</sup>H NMR spectrum and calculate the reaction conversion.

Computations. Calculations were performed at the Minnesota Supercomputing Institute using the Gaussian 16 software package. Geometry optimizations were carried out with the M06-2X density functional. <sup>27</sup><sup>1</sup>–<sup>29</sup> Cations were first explored with the 3-21G basis set, and the resulting structures were reoptimized with the cc-pVDZ and then the aug-cc-pVDZ basis sets.<sup>31</sup> Vibrational frequencies were computed for the final structures to confirm that they correspond to energy minima (no negative eigenvalues), and obtain ZPEs, thermal corrections to the enthalpies at 298 K, and entropies. Unscaled vibrational frequencies were used to derive the resulting thermochemical data, and small frequencies that contribute more than 0.5RT to the enthalpy correction were replaced by 0.5RT. For the tetrakis(3,5-dimethoxyphenyl)phosphonium ion and P4-t-Bu·H+, the optimizations with the augmented basis set proved difficult to carry out, so cc-pVDZ vibrational frequencies and aug-cc-pVDZ singlepoint energies were used. This approach was benchmarked with  $Ph_4P^+$  and found to have little effect on the final energy (<0.1 kcal mol<sup>-1</sup>). For the cryptand complex, the aug-cc-pVDZ-X2C basis set was used for K+.86

Geometries for the chloride salts were obtained by carrying out multiple optimizations with Cl<sup>-</sup> placed at different locations. In general, the chloride anion was located at different positions where it could interact with the cation via favorable C–H··Cl<sup>-</sup> interactions, but a few optimizations were also carried out in which chloride was placed 4–10 Å away from the cation. All of the distant starting structures converged to species that closely matched those obtained via chemical intuition. The same series of basis sets were used as for the cations [i.e., 3-21G, cc-pVDZ, and aug-cc-pVDZ (aug-cc-pVDZ-X2C for K<sup>+</sup>)], and the vibrational frequencies for the aug-cc-pVDZ

structures were found to have no imaginary frequencies, indicating that they correspond to energy minima. Single-point DCM solvation calculations were subsequently carried out on the aug-cc-pVDZ optimized phosphonium ions and their chloride salts using the aug-cc-pVTZ basis set and the CPCM solvation model.  $^{33,34}$  Single-point energies including the effects of dispersion were also computed using the M06-2X functional and the aug-cc-pVDZ basis set with Grimme's original D3 damping function.  $^{35}$  In addition, the use of the  $\omega$ B97X-D,  $^{36}$  M11,  $^{37}$  and MN15 density functionals were explored using the M06-2X optimized structures. In select cases, MN15 optimizations and vibrational frequencies were also computed. Calculated structures were assembled in the figures using the CylView application.  $^{87}$ 

#### ASSOCIATED CONTENT

#### **Data Availability Statement**

Data Availability Statement: The data underlying this study are available in the published article and its online Supporting Information.

#### **Solution** Supporting Information

The Supporting Information is available free of charge at https://pubs.acs.org/doi/10.1021/acs.joc.2c02001.

Kinetic data, NMR and IR spectra, computed structures and energies, ion-pairing equilibrium constants, and the complete citation to ref 85 (PDF)

#### AUTHOR INFORMATION

#### **Corresponding Author**

Steven R. Kass — Department of Chemistry, University of Minnesota, Minneapolis, Minnesota 55455, United States; orcid.org/0000-0001-7007-9322; Email: kass@umn.edu

#### **Author**

Stephen H. Dempsey – Department of Chemistry, University of Minnesota, Minneapolis, Minnesota 55455, United States

Complete contact information is available at: https://pubs.acs.org/10.1021/acs.joc.2c02001

#### Notes

The authors declare no competing financial interest.

#### ACKNOWLEDGMENTS

We thank Mr. David Freytag for carrying out supplemental conformational searches on tetraarylphosphonium chlorides and Mr. David Detloff for his synthetic assistance. Generous support from the National Science Foundation (CHE-1955186), the donors of the American Chemical Society Petroleum Research Fund (ACS PRF 65096-ND4), and the Minnesota Supercomputing Institute for Advanced Computational Research is also gratefully acknowledged.

#### REFERENCES

- (1) Strauss, S. H. The Search for Larger and More Weakly Coordinating Anions. *Chem. Rev.* **1993**, 93, 927–942.
- (2) Krossing, I.; Raabe, I. Noncoordinating Anions—Fact or Fiction? A Survey of Likely Candidates. *Angew. Chem., Int. Ed.* **2004**, 43, 2066–2090.
- (3) Riddlestone, I. M.; Kraft, A.; Schaefer, J.; Krossing, I. Taming the Cationic Beast: Novel Developments in the Synthesis and Application of Weakly Coordinating Anions. *Angew. Chem., Int. Ed.* **2018**, *57*, 13982–14024.
- (4) Douvris, C.; Ozerov, O. V. Hydrodefluorination of Perfluoroalkyl Groups Using Silylium-Carborane Catalysts. *Science* **2008**, *321*, 1188–1190.

- (5) Popov, S.; Shao, B.; Bagdasarian, A. L.; Benton, T. R.; Zou, L.; Yang, Z.; Houk, K. N.; Nelson, H. M. Teaching an Old Carbocation New Tricks: Intermolecular C-H Insertion Reactions of Vinyl Cations. *Science* **2018**, *361*, 381–387.
- (6) Wigman, B.; Popov, S.; Bagdasarian, A. L.; Shao, B.; Benton, T. R.; Williams, C. G.; Fisher, S. P.; Lavallo, V.; Houk, K. N.; Nelson, H. M. Vinyl Carbocations Generated under Basic Conditions and Their Intramolecular C-H Insertion Reactions. *J. Am. Chem. Soc.* **2019**, *141*, 9140–9144.
- (7) Kitazawa, Y.; Takita, R.; Yoshida, K.; Muranaka, A.; Matsubara, S.; Uchiyama, M. Naked" Lithium Cation: Strongly Activated Metal Cations Facilitated by Carborane Anions. *J. Org. Chem.* **2017**, 82, 1931–1935.
- (8) Adet, N.; Specklin, D.; Gourlaouen, C.; Damiens, T.; Jacques, B.; Wehmschulte, R. J.; Dagorne, S. Towards Naked Zinc(II) in the Condensed Phase: A Highly Lewis Acidic Zn II Dication Stabilized by Weakly Coordinating Carborate Anions. *Angew. Chem., Int. Ed.* **2021**, 60, 2084–2088.
- (9) Xie, Z.; Bau, R.; Reed, C. A. Free" [Fe(Tpp)]+ Cation: A New Concept in the Search for the Least Coordinating Anion. *Angew. Chem., Int. Ed.* **1995**, 33, 2433–2434.
- (10) Reed, C. A. Carboranes: A New Class of Weakly Coordinating Anions for Strong Electrophiles, Oxidants, and Superacids. *Acc. Chem. Res.* **1998**, *31*, 133–139.
- (11) Xie, Z.; Jelinek, T.; Bau, R.; Reed, C. A. New Weakly Coordinating Anions. III. Useful Silver and Trityl Salt Reagents of Carborane Anions. *J. Am. Chem. Soc.* **1994**, *116*, 1907–1913.
- (12) Juhasz, M.; Hoffmann, S.; Stoyanov, E.; Kim, K. C.; Reed, C. A. The Strongest Isolable Acid. *Angew. Chem., Int. Ed.* **2004**, *43*, 5352–5355.
- (13) Reed, C. A.; Xie, Z.; Bau, R.; Benesi, A. Closely Approaching the Silylium Ion (R 3 Si + ). *Science* **1993**, 262, 402–404.
- (14) Türp, D.; Wagner, M.; Enkelmann, V.; Müllen, K. Synthesis of Nanometer-Sized, Rigid, and Hydrophobic Anions. *Angew. Chem., Int. Ed.* **2011**, *50*, 4962–4965.
- (15) Cacciapaglia, R.; Mandolins, L. Catalysis by Metal Ions in Reactions of Crown Ether Substrates. *Chem. Soc. Rev.* **1993**, 22, 221–231.
- (16) Gokel, G. W.; Leevy, W. M.; Weber, M. E. Crown Ethers: Sensors for Ions and Molecular Scaffolds for Materials and Biological Models. *Chem. Rev.* **2004**, *104*, 2723–2750.
- (17) Landini, D.; Maia, A.; Montanari, F.; Tundo, P. Lipophilic [2.2.2] Cryptands as Phase-Transfer Catalysts. Activation and Nucleophilicity of Anions in Aqueous-Organic Two-Phase Systems and in Organic Solvents of Low Polarity. *J. Am. Chem. Soc.* **2002**, *101*, 2526–2530.
- (18) Von Zelewsky, A. Stereochemistry of Coordination Compounds; John Wiley: Chichester, 1995; pp 1–254.
- (19) Lehn, J. M. Supramolecular Chemistry: Concepts and Perspectives; VCH: Weinheim, 1995; pp 1–271.
- (20) Schwesinger, R.; Schlemper, H.; Hasenfratz, C.; Willaredt, J.; Dambacher, T.; Breuer, T.; Ottaway, C.; Fletschinger, M.; Boele, J.; Fritz, H.; Putzas, D.; Rotter, H. W.; Bordwell, F. G.; Satish, A. V.; Ji, G. Z.; Peters, E. M.; Peters, K.; Von Schnering, H. G.; Walz, L. Extremely Strong, Uncharged Auxiliary Bases; Monomeric and Polymer-Supported Polyaminophosphazenes (P2-P5). *Liebigs Ann. Chem.* 1996, 1996, 1055–1081.
- (21) Schwesinger, R.; Link, R.; Wenzl, P.; Kossek, S. Anhydrous Phosphazenium Fluorides as Sources for Extremely Reactive Fluoride Ions in Solution. *Chem.—Eur. J.* **2005**, *12*, 438–445.
- (22) Prat, J. R.; Gaggioli, C. A.; Cammarota, R. C.; Bill, E.; Gagliardi, L.; Lu, C. C. Bioinspired Nickel Complexes Supported by an Iron Metalloligand. *Inorg. Chem.* **2020**, *59*, 14251–14262.
- (23) Ruff, J. K.; Schlientz, W. J.; Dessy, R. E.; Malm, J. M.; Dobson, G. R.; Memering, M. N.  $\mu$ -Nitridobis(Triphenylphosphorus)(1+) ("PPN") Salts with Metal Carbonyl Anions. *Inorganic Syntheses*; McGraw-Hill Inc., 2007; Vol. 15, pp 84–90.
- (24) Nacsa, E. D.; Lambert, T. H. Higher-Order Cyclopropenimine Superbases: Direct Neutral Brønsted Base Catalyzed Michael

- Reactions with  $\alpha$ -Aryl Esters. J. Am. Chem. Soc. **2015**, 137, 10246–10253.
- (25) Bandar, J. S.; Tanaset, A.; Lambert, T. H. Phase-Transfer and Other Types of Catalysis with Cyclopropenium Ions. *Chem.—Eur. J.* **2015**, *21*, 7365–7368.
- (26) Bandar, J. S.; Barthelme, A.; Mazori, A. Y.; Lambert, T. H. Structure—Activity Relationship Studies of Cyclopropenimines as Enantioselective Brønsted Base Catalysts. *Chem. Sci.* **2015**, *6*, 1537—1547.
- (27) Zhao, Y.; Truhlar, D. G. How Well Can New-Generation Density Functionals Describe the Energetics of Bond-Dissociation Reactions Producing Radicals? *J. Phys. Chem. A* **2008**, *112*, 1095–1099
- (28) Zhao, Y.; Truhlar, D. G. The M06 suite of density functionals for main group thermochemistry, thermochemical kinetics, noncovalent interactions, excited states, and transition elements: two new functionals and systematic testing of four M06-class functionals and 12 other functionals. *Theor. Chem. Acc.* 2008, 120, 215–241.
- (29) Zhao, Y.; Truhlar, D. G. Density Functionals with Broad Applicability in Chemistry. Acc. Chem. Res. 2008, 41, 157–167.
- (30) Ditchfield, R.; Hehre, W. J.; Pople, J. A. Self-Consistent Molecular-Orbital Methods. IX. An Extended Gaussian-Type Basis for Molecular-Orbital Studies of Organic Molecules. *J. Chem. Phys.* **1971**, *54*, 724–728.
- (31) Dunning, T. H., Jr. Gaussian basis sets for use in correlated molecular calculations. I. The atoms boron through neon and hydrogen. *J. Chem. Phys.* **1989**, *90*, 1007–1023.
- (32) Basis set superposition errors (BSSEs) were computed using the counterpoise method but are omitted from the given results since these corrections were found to only amount to 0.4–0.9 kcal mol<sup>-1</sup>.
- (33) Barone, V.; Cossi, M. Quantum Calculation of Molecular Energies and Energy Gradients in Solution by a Conductor Solvent Model. *J. Phys. Chem. A* **1998**, *102*, 1995–2001.
- (34) Cossi, M.; Rega, N.; Scalmani, G.; Barone, V. Energies, Structures, and Electronic Properties of Molecules in Solution with the C-PCM Solvation Model. *J. Comput. Chem.* **2003**, 24, 669–681.
- (35) Grimme, S.; Antony, J.; Ehrlich, S.; Krieg, H. A Consistent and Accurate Ab Initio Parametrization of Density Functional Dispersion Correction (DFT-D) for the 94 Elements H-Pu. *J. Chem. Phys.* **2010**, 132, 154104.
- (36) Chai, J.-D.; Head-Gordon, M. Long-Range Corrected Hybrid Density Functionals with Damped Atom-Atom Dispersion Corrections. *Phys. Chem. Chem. Phys.* **2008**, *10*, 6615–6620.
- (37) Peverati, R.; Truhlar, D. G. Improving the Accuracy of Hybrid Meta-GGA Density Functionals by Range Separation. *J. Phys. Chem. Lett.* **2011**, *2*, 2810–2817.
- (38) Yu, H. S.; He, X.; Li, S. L.; Truhlar, D. G. MN15: A Kohn-Sham Global-Hybrid Exchange-Correlation Density Functional with Broad Accuracy for Multi-Reference and Single-Reference Systems and Noncovalent Interactions. *Chem. Sci.* **2016**, *7*, 5032–5051.
- (39) Fry, A. J. Computational Studies of Ion Pairing. 10. Ion Pairing between Tetrabutylammonium Ion and Inorganic Ions: A General Motif Confirmed. *J. Org. Chem.* **2015**, *80*, 3758–3765.
- (40) Hehre, W.; Radom, L.; Schleyer, P. v. R.; Pople, J. Ab Initio Molecular Theory; John Wiley & Sons: New York, 1986; p 548.
- (41) Jensen, J. H.; Gordon, M. S. On the Number of Water Molecules Necessary To Stabilize the Glycine Zwitterion. *J. Am. Chem. Soc.* **1995**, 117, 8159–8170.
- (42) Allerhand, A.; Von Rague Schleyer, P. v. R. A Survey of C-H Groups as Proton Donors in Hydrogen Bonding. *J. Am. Chem. Soc.* **1963**, *85*, 1715–1723.
- (43) Kwak, K.; Rosenfeld, D. E.; Chung, J. K.; Fayer, M. D. Solute-Solvent Complex Switching Dynamics of Chloroform between Acetone and Dimethylsulfoxide-Two-Dimensional IR Chemical Exchange Spectroscopy. *J. Phys. Chem. B* **2008**, *112*, 13906–13915.
- (44) Arunan, E.; Desiraju, G. R.; Klein, R. A.; Sadlej, J.; Scheiner, S.; Alkorta, I.; Clary, D. C.; Crabtree, R. H.; Dannenberg, J. J.; Hobza, P.; Kjaergaard, H. G.; Legon, A. C.; Mennucci, B.; Nesbitt, D. J.

- Definition of the Hydrogen Bond (IUPAC Recommendations 2011). *Pure Appl. Chem.* **2011**, *83*, 1637–1641.
- (45) Shirakawa, S.; Liu, S.; Kaneko, S.; Kumatabara, Y.; Fukuda, A.; Omagari, Y.; Maruoka, K. Tetraalkylammonium Salts as Hydrogen-Bonding Catalysts. *Angew. Chem., Int. Ed.* **2015**, *54*, 15767–15770.
- (46) Kumatabara, Y.; Kaneko, S.; Nakata, S.; Shirakawa, S.; Maruoka, K. Hydrogen-Bonding Catalysis of Tetraalkylammonium Salts in an Aza-Diels-Alder Reaction. *Chem.—Asian J.* **2016**, *11*, 2126–2129.
- (47) Payne, C.; Kass, S. R. Structural Considerations for Charge-Enhanced Brønsted Acid Catalysts. *J. Phys. Org. Chem.* **2020**, 33, No. e4069.
- (48) Schwesinger, R.; Link, R.; Thiele, G.; Rotter, H.; Honert, D.; Limbach, H.-H.; Männle, F. Stable Phosphazenium Ions in Synthesis—an Easily Accessible, Extremely Reactive "Naked" Fluoride Salt. *Angew. Chem., Int. Ed.* **1991**, *30*, 1372–1375.
- (49) Shokri, A.; Wang, X.-B.; Wang, Y.; O'Doherty, G. A.; Kass, S. R. Flexible Acyclic Polyol-Chloride Anion Complexes and Their Characterization by Photoelectron Spectroscopy and Variable Temperature Binding Constant Determinations. *J. Phys. Chem. A* **2016**, *120*, 1661–1668.
- (50) Samet, M.; Buhle, J.; Zhou, Y.; Kass, S. R. Charge-Enhanced Acidity and Catalyst Activation. *J. Am. Chem. Soc.* **2015**, *137*, 4678–4680.
- (51) Thordarson, P. Determining Association Constants From Titration Experiments in Supramolecular Chemistry. *Chem. Soc. Rev.* **2011**, *40*, 1305–1323.
- (52) Brynn Hibbert, D.; Thordarson, P. The Death of the Job Plot, Transparency, Open Science and Online Tools, Uncertainty Estimation Methods and Other Developments in Supramolecular Chemistry Data Analysis. *Chem. Commun.* **2016**, *52*, 12792–12805.
- (53) Alunni, S.; Pero, A.; Reichenbach, G. Reactivity of Ions and Ion Pairs in the Nucleophilic Substitution Reaction on Methyl p-Nitrobenzenesulfonate. *J. Chem. Soc., Perkin Trans.* **1998**, *2*, 1747–1750.
- (54) Sessler, J. L.; Gross, D. E.; Cho, W.-S.; Lynch, V. M.; Schmidtchen, F. P.; Bates, G. W.; Light, M. E.; Gale, P. A. Calix[4]pyrrole as a Chloride Anion Receptor: Solvent and Effects, 2006 Countercation Effects. J. Am. Chem. Soc. 2006, 128, 12281–12288.
- (55) Shokri, A.; Kass, S. R. Solvent Effects on the Molecular Recognition of Anions. *Chem. Commun.* **2013**, *49*, 11674–11676.
- (56) Omission of the 3,5-Me<sub>2</sub>Phos chloride salt from the least-square analysis affords  $\Delta H_{\rm D}^{\circ}$  (kcal mol<sup>-1</sup>) = -5.91 × ln k + 49.1,  $r^2$  = 0.91, and steric interactions may be responsible for its deviation from the line
- (57) Rocchigiani, L.; Bellachioma, G.; Ciancaleoni, G.; Crocchianti, S.; Laganà, A.; Zuccaccia, C.; Zuccaccia, D.; Macchioni, A. Anion-Dependent Tendency of Di-Long-Chain Quaternary Ammonium Salts to Form Ion Quadruples and Higher Aggregates in Benzene. *ChemPhysChem* **2010**, *11*, 3243–3254.
- (58) Hack, J.; Grills, D. C.; Miller, J. R.; Mani, T. Identification of Ion-Pair Structures in Solution by Vibrational Stark Effects. *J. Phys. Chem. B* **2016**, *120*, 1149–1157.
- (59) Hefter, G. When spectroscopy fails: The measurement of ion pairing. *Pure Appl. Chem.* **2006**, *78*, 1571–1586.
- (60) Pregosin, P. S. Applications of NMR diffusion methods with emphasis on ion pairing in inorganic chemistry: a mini-review. *Magn. Reson. Chem.* **2016**, *55*, 405–413.
- (61) Hogen-Esch, T. E.; Smid, J. Studies of Contact and Solvent-Separated Ion Pairs of Carbanions. I. Effect of Temperature, Counterion, and Solvent. J. Am. Chem. Soc. 1966, 88, 307–318.
- (62) Hogen-Esch, T. E.; Smid, J. Studies of Contact and Solvent-Separated Ion Pairs of Carbanions. II. Conductivities and Thermodynamics of Dissociation of Fluorenyllithium, -sodium, and -cesium. J. Am. Chem. Soc. 1966, 88, 318–324.
- (63) Ellingsen, T.; Smid, J. Studies of Contact and Solvent-Separated Ion Pairs of Carbanions. VI. Conductivities and Thermodynamics of

- Dissociation of Fluorenyl Alkali Salts in Tetrahydrofuran and Dimethoxyethane. J. Phys. Chem. 1969, 73, 2712–2719.
- (64) Smid, J. The Discovery of Two Kinds of Ion Pairs. *J. Polym. Sci., Polym. Chem.* **2004**, 42, 3655–3667.
- (65) Reich, H. J.; Sikorski, W. H.; Thompson, J. L.; Sanders, A. W.; Jones, A. C. Interconversion of Contact and Separated Ion Pairs in Silyl- and Arylthio-Substituted Alkyllithium Reagents. *Org. Lett.* **2006**, *8*, 4003–4006.
- (66) Reich, H. J.; Sikorski, W. H.; Sanders, A. W.; Jones, A. C.; Plessel, K. N. Multinuclear NMR Study of the Solution Structure and Reactivity of Tris(trimethylsilyl)methyllithium and its Iodine Ate Complex. J. Org. Chem. 2009, 74, 719–729.
- (67) Krom, J. A.; Streitwieser, A. Kinetics of Methylation of a Cesium Enolate in THF. The Importance of the Free Enolate Ion in an Aggregated System. *J. Am. Chem. Soc.* **1992**, *114*, 8747–8748.
- (68) Ellington, J. C., Jr.; Arnett, E. M. Kinetics and Thermodynamics of Phenolate Silylation and Alkylation. *J. Am. Chem. Soc.* **1988**, *110*, 7778–7785 Reactivity varies with aggregation and ion pairing.
- (69) Reich, H. J.; Sanders, A. W.; Fiedler, A. T.; Bevan, M. J. The Effect of HMPA on the Reactivity of Epoxides, Aziridines, and Alkyl Halides with Organolithium Reagents. *J. Am. Chem. Soc.* **2002**, *124*, 13386–13387.
- (70) Liu, Y.; Sengupta, A.; Raghavachari, K.; Flood, A. H. Anion Binding in Solution: Beyond the Electrostatic Regime. *Chem* **2017**, *3*, 411–427.
- (71) Martin, R. B. Comparisons of indefinite self-association models. *Chem. Rev.* **1996**, *96*, 3043–3064.
- (72) Equation 3 represents a simplified and idealized view of the species involved in the dilution experiment since aggregates, among other species, undoubtedly play a role over a wide concentration range.
- (73) Preliminary Arrhenius plots based upon rate determinations from 5 to 35  $^{\circ}$ C for PPN, PPh<sub>4</sub>, 4-Me<sub>2</sub>NPhos, and 3,5-(MeO)<sub>2</sub>Phos, are nonlinear. This is consistent with the presence of more than one reactive species.
- (74) A similar dilution study was carried out for  $Ph_4PCl$  in  $CDCl_3$ , which has a lower dielectric constant than  $CD_2Cl_2$ . A poor nonlinear fit of the data at low (<1 mM) concentrations was obtained suggestive of the presence of higher-order aggregates. Application of a different binding model, CoEK aggregation, however, provides a good fit of the data and  $K_{ip} = 2.19 \times 10^3 \pm 5.8\%$  M $^{-1}$ . See the Supporting Information and the following references for additional information. (a) Thordarson, P.; Sewell, K.; Efremova, V. Bindfit v0.5. www. supramolecular.org (accessed Aug 14, 2022). (b) Evstigneev, M. P.; Buchelnikov, A. S.; Kostjukov, V. V.; Pashkova, I. S.; Evstigneev, V. P. Indistinguishability of the Models of Molecular Self-Assembly. Supramol. Chem. 2013, 25, 199–203.
- (75) Shao, B.; Bagdasarian, A. L.; Popov, S.; Nelson, H. M. Arylation of Hydrocarbons Enabled by Organosilicon Reagents and Weakly Coordinating Anions. *Science* **2017**, *355*, 1403–1407.
- (76) Yonemoto-Kobayashi, M.; Inamoto, K.; Kondo, Y. Desilylative Carboxylation of Aryltrimethylsilanes Using CO2 in the Presence of Catalytic Phosphazenium Salt. *Chem. Lett.* **2014**, 43, 477–479.
- (77) Hong, C. M.; Whittaker, A. M.; Schultz, D. M. Nucleophilic Fluorination of Heteroaryl Chlorides and Aryl Triflates Enabled by Cooperative Catalysis. *J. Org. Chem.* **2021**, *86*, 3999–4006.
- (78) Harris, R. K.; Becker, E. D.; Cabral de Menezes, S. M.; Goodfellow, R.; Granger, P. NMR Nomenclature. Nuclear Spin Properties and Conventions for Chemical Shifts (IUPAC Recommendations 2001). *Pure Appl. Chem.* **2001**, 73, 1795–1818.
- (79) Rosenau, C. P.; Jelier, B. J.; Gossert, A. D.; Togni, A. Exposing the Origins of Irreproducibility in Fluorine NMR Spectroscopy. *Angew. Chem., Int. Ed.* **2018**, *57*, 9528–9533.
- (80) Volz, H.; Ruchti, L. Ein Beitrag zum Mechanismus der Polonovski-Reaktion. *Justus Liebigs Ann. Chem.* **1972**, 763, 184–197. (81) Hammond, G. S.; Warkentin, J. The Addition of Deuterium Bromide to 1,3-Cyclohexadiene. *J. Am. Chem. Soc.* **1961**, 83, 2554–2559.

- (82) Grushin, V. V.; Tolstaya, T. P.; Lisichkina, I. N.; Grishin, Y. K.; Shcherbina, T. M.; Kampel, V. T.; Bregadze, V. I.; Godovikov, N. N. Reaction of B-Halonium Derivatives of Carboranes-12 with Triphenylphosphine. *Bull. Acad. Sci. USSR, Div. Chem. Sci.* 1983, 32, 429–431.
- (83) Manandhar, R.; Rath, N. P.; Jones, M. W. Bis-(Triphenylphosphine)Iminium Tetrafluoroborate Chloroform Monosolvate. *IUCrData* **2018**, *3*, x181108.
- (84) Link, R. Extrem Reaktive Organische Fluoride-Salze Synthese Und Anwendungen. Ph.D. Thesis, Albert-Ludwigs-Universität Freiburg im Bresgau, 1995, pp 1–247.
- (85) Frisch, M. J.; Trucks, G. W.; Schlegel, H. B.; Scuseria, G. E.; Robb, M. A.; et al. *Gaussian 16*; Gaussian, Inc.: Wallingford CT, 2016.
- (86) Hill, J. G.; Peterson, K. A. Gaussian basis sets for use in correlated molecular calculations. XI. Pseudopotential-based and allelectron relativistic basis sets for alkali metal (K-Fr) and alkaline earth (Ca-Ra) elements. *J. Chem. Phys.* **2017**, *147*, 244106.
- (87) Legault, C. Y. CYLview20. Université de Sherbrooke, 2020. (http://www.cylview.org (accessed Aug 14, 2022)

### **□** Recommended by ACS

## Absolute Hydration Free Energy of Small Anions and the Aqueous $pK_a$ of Simple Acids

Ashley S. McNeill, David A. Dixon, et al.

DECEMBER 05, 2022

THE JOURNAL OF PHYSICAL CHEMISTRY A

READ 🗹

## Divalent Benzimidazolium-Based Axles for Self-Reporting Pseudorotaxanes

S. Maryamdokht Taimoory, John F. Trant, et al.

NOVEMBER 15, 2022

THE JOURNAL OF ORGANIC CHEMISTRY

READ 🗹

## Sodium Isopropyl(trimethylsilyl)amide: A Stable and Highly Soluble Lithium Diisopropylamide Mimic

Yun Ma, David B. Collum, et al.

OCTOBER 25, 2022

THE JOURNAL OF ORGANIC CHEMISTRY

READ 🗹

# Synthesis of a Bench-Stable Manganese(III) Chloride Compound: Coordination Chemistry and Alkene Dichlorination

Ananya Saju, David C. Lacy, et al.

SEPTEMBER 06, 2022

JOURNAL OF THE AMERICAN CHEMICAL SOCIETY

READ 🗹

Get More Suggestions >